# DEVELOPMENT AND CHARACTERIZATION OF NANOPARTICLES MODIFIED UREA FORMALDEHYDE RESIN ADHESIVE

**BY**

**DANIEL, Emmanuel**
**M.Eng/SEET/2017/7300**

**A THESIS SUBMITTED TO THE POSTGRADUATE SCHOOL FEDERAL UNIVERSITY OF TECHNOLOGY, MINNA, NIGERIA IN PARTIAL FULFILMENT OF THE REQUIREMENTS FOR THE AWARD OF THE DEGREE OF MASTER OF ENGINEERING (M.Eng) IN CHEMICAL ENGINEERING**

**OCTOBER, 2021**

## ABSTRACT

Urea formaldehyde resin lack in water resistance owing to the low stability of the amino-methylene bond making it susceptible to hydrolysis and thus limiting its use to interiors only. The aim of this study is to modify Urea Formaldehyde resin using nanoparticles derived from bamboo waste and its application in particleboard production. Biochar was produced from pyrolysis of waste bamboo at temperatures of 400 $^{o}$C, 450 $^{o}$C and 500 $^{o}$C. Size reduction of the biochars produced was carried out using a ball mill for 1 hr. The particle size analysis showed that the particles were wide and dispersed having average sizes of particles between 40 to 60 diameter nanometer (d.nm). Physical properties of bamboo and nano biochar were evaluated, moisture content and volatile matter decreased with increase in pyrolysis temperature while ash content and fixed carbon increased with increase in pyrolysis temperature. Chemical properties were also evaluated, percentage carbon content of 54.82 %, 55.62 % and 56.48 % respectively increased with increase in pyrolysis temperature while percentage hydrogen and oxygen decreased with increase in pyrolysis temperature. The percentage nitrogen content was very low ranging from 0.22 to 0.24 % which implies very little pollution from $NO_x$ species that might be formed. Urea formaldehyde resin adhesive was synthesized using the alkaline-acid method and modified using the produced nano biochars. Physical and chemical properties of the neat and modified UF resins were evaluated. The viscosities of the modified resins increased to 152 cP, 151 cP and 154 cP respectively as against the neat resin which had a viscosity of 150 cP. The solid content also increased significantly ranging from 63-65 % for modified resins while the neat resin had a solid content of 60 %. Gel time, density and pH of both neat and modified resins did not change significantly with gel time ranging between 58 to 60 sec, densities of between 1.28 to 1.35 g/cm$^3$ and pH ranging from 7.8 to 8.0. The neat and modified UF resins were used to produce particleboards using saw dust as filler. Physical and mechanical properties of the particleboards were evaluated, the densities of particleboards were within the range of 0.68 g/cm$^3$ and 0.79 g/cm$^3$ which implies that they were low density particleboards. Particleboard modified with sample UF2 showed the highest water resistance and least thickness swell of 32.13 % and 40.00 % respectively. It also showed the highest values in tensile strength of 25.16 MPa and elastic modulus of 19.83 MPa. Particleboards produced with sample UF3 gave the highest hardness of 44.9 HV and impact energy of 0.32 J. The findings presented demonstrate that nano biochar derived from bamboo wastes presents suitable properties that can be used in the modification of UF resin. Particleboard produced with the modified UF resin significantly improved in its water resistance, thickness swell, tensile strength and elastic modulus.

## TABLE OF CONTENTS


Title page i

Declaration ii

Certification iii

Acknowledgments iv

Abstract v

Table of Content vi

List of Tables xii

List of Figures xiii

List of Plates xiv

List of Abbreviations xv

**CHAPTER ONE**

**1.0 INTRODUCTION** 1

1.1 Background to the Study 1

1.2 Statement of the Research Problem 4

1.3 Aim and Objectives of the Study 4

1.4 Justification of the Study 4

1.5 Scope of the Study 5

**CHAPTER TWO**

**2.0 LITERATURE REVIEW** 6

2.1 Adhesives 6

2.2 Properties of Adhesives 6

2.2.1 Viscosity 6

2.2.2 Gelation time 7

2.2.3 Density 7

2.3 Applications of Adhesives 7

2.4 Resins 9

2.4.1 Types of resins 10

2.4.1.1 Thermoplastic resins 10

2.4.1.2 Thermosetting resins 10

2.5 Urea formaldehyde 11

2.6 Composites 13

2.7 Particleboard 15

2.7.1 Properties of particleboard 19

2.7.1.1 Density 19

2.7.1.2 Water absorption 20

2.7.1.3 Thickness swelling 20

2.7.1.4 Hardness 20

2.7.1.5 Impact toughness 21

2.7.1.6 Tensile properties 21

2.8 Biomass 22

2.9 Bamboo 23

2.9.1 Uses of bamboo 24

2.10 Biochar 25

2.11 Pyrolysis 26

2.11.1 Basic principle of pyrolysis 27

2.11.2 Types of pyrolysis 28

2.11.2.1 Slow pyrolysis 28

2.11.2.2 Fast pyrolysis 28

2.11.2.3 Flash pyrolysis 28

2.12 Nanotechnology 30

2.13 Nanoparticles 30

2.13.1 Synthesis of nanoparticles 31

2.13.1.1 Bottom-up approaches 31

2.13.1.2 Top-down approaches 31

2.14 Ball Milling 32

2.15 Application of Nanotechnology in the Wood Industry 33

**CHAPTER THREE**


**3.0 RESEARCH METHODOLOGY** 34

3.1 Materials and Equipment 34

3.2 Methodology 36

3.2.1 Sample collection and preparation 36

3.2.2 TGA of bamboo 36

3.2.3 Pyrolysis of bamboo 36

3.2.4 Physicochemical analysis 37

3.2.5 Proximate analysis 37

3.2.5.1 Moisture content 37

3.2.5.2 Ash content 37

3.2.5.3 Volatile matter 38

3.2.5.4 Fixed carbon content 38

3.2.6 Ultimate Analysis 38

3.2.7 Preparation of nanoparticles 39

3.2.8 Particle size analysis 39

3.2.9 Preparation of urea formaldehyde resin 39

3.2.10 Modification of urea formaldehyde resin 41

3.2.11 Particleboard production 41

3.2.11.1 Particles preparation 41

3.2.11.2 Particleboard formation and pressing 41

3.2.12 Physical and mechanical properties of particleboard 42

3.2.12.1 Density 42

3.2.12.2 Water absorption 42

3.2.12.3 Thickness swelling 43

3.2.12.4 Tensile test 43

3.2.12.5 Hardness test 44

3.2.12.6 Impact test 44

3.2.13 Thermal analysis (TGA) 45

3.2.14 Fourier transform infrared (FTIR) 46

**CHAPTER FOUR**

**4.0 RESULTS AND DISCUSSION** 47

4.1 Thermal Analysis of Bamboo 47

4.2 Characterization of Bamboo 49

4.3 Proximate and Ultimate Analysis of Bamboo 49

4.4 Proximate and Ultimate Analysis of Biochar 50

4.5 Particle size Analysis of Biochar 51

4.6 FTIR Spectroscopy of Biochar 52

4.7 Physicochemical Properties of Urea Formaldehyde Resin 55

4.8 Thermal Analysis of Urea Formaldehyde Resin 56

4.9 FTIR Spectroscopy of Urea Formaldehyde Resin 58

4.10 Physical and Mechanical properties of particleboards 59

4.10.1 Density 59

4.10.2 Water absorption 60

4.10.3 Thickness swelling 61

4.10.4 Tensile strength 62

4.10.5 Elastic modulus 63

4.10.6 Elongation 64

4.10.7 Hardness test 65

4.10.8 Impact test 66

**CHAPTER FIVE**

**5.0 CONCLUSION AND RECOMMENDATIONS** 68

5.1 Conclusion 68

5.2 Recommendations 69

5.3 Contribution to Knowledge 70

**REFERENCES** 71

**APPENDICES** 77

## LIST OF TABLES


| Table | Title | Page |
|---|---|---|
| 2.1 | Types of Pyrolysis | 29 |
| 3.1 | List of Materials Used For Experiment | 34 |
| 3.2 | List of Equipment Used For Experiment | 35 |
| 3.3 | Resin Formulation | 41 |
| 3.4 | Particleboard Formation | 41 |
| 4.1 | Composition of Bamboo | 49 |
| 4.2 | Proximate Analysis of Bamboo | 50 |
| 4.3 | Ultimate Analysis of Bamboo | 50 |
| 4.4 | Proximate Analysis of Biochar | 51 |
| 4.5 | Ultimate Analysis of Biochar | 51 |
| 4.6 | Classification of Functional Groups of Bamboo and Nanobiochar | 54 |
| 4.7 | Physicochemical Properties of Neat and Modified UF Resin | 55 |
| 4.8 | Classification of Functional Groups of Neat and Modified UF Resin | 59 |
| 4.9 | Densities of Neat and Modified Particleboards | 59 |

## LIST OF FIGURES


| Figure | Title | Page |
|---|---|---|
| 4.1 | TGA of Bamboo | 47 |
| 4.2 | DTA of Bamboo | 48 |
| 4.3 | Particle Size Distribution of Biochar | 52 |
| 4.4 | FTIR Spectra for Bamboo and Nano Biochar | 53 |
| 4.5 | TGA of Neat and Modified UF Resin | 56 |
| 4.6 | DTA of Neat and Modified UF Resin | 57 |
| 4.7 | FTIR Spectra for Neat and Modified UF resin | 58 |
| 4.8 | Water Absorption of Neat and Modified Particleboards | 60 |
| 4.9 | Thickness Swelling of Neat and Modified Particleboards | 61 |
| 4.10 | Tensile Strength of Neat and Modified Particleboards | 62 |
| 4.11 | Elastic Modulus of Neat and Modified Particleboards | 63 |
| 4.12 | Elongation of Neat and Modified Particleboards | 64 |
| 4.13 | Hardness of Neat and Modified Particleboards | 65 |
| 4.14 | Impact Strength of Neat and Modified Particleboards | 66 |

## LIST OF PLATES


| Plate | Title | Page |
|---|---|---|
| I | Structures of Urea and Formaldehyde | 12 |
| II | Urea Formaldehyde Formation | 13 |
| III | Saw dust for Particleboard Production | 16 |
| IV | Metal Mould Plate | 17 |
| V | Compression Mould Machine | 18 |
| VI | Typical pictures of Particleboards | 19 |
| VII | Bamboo stems | 24 |
| VIII | Typical picture of Biochar | 26 |
| IX | Flow Diagram of a Typical Pyrolysis Unit | 27 |
| X | Methods of Nanomaterial synthesis | 32 |

## LIST OF ABBREVIATIONS

Urea Formaldehyde (UF)

Fourier Transform Infrared (FTIR)

Thermogravimetric analysis (TGA)

Differential Thermal analysis (DTA)

American Society for Testing and Materials (ASTM)

Japanese Industrial Standards (JIS)

# CHAPTER ONE

## 1.0 INTRODUCTION

### 1.1 Background to the Study

Urea-formaldehyde (UF) resin is extensively used as a binder adhesive for the production of wood-based panels such as medium density fiberboard, particleboard (PB) and hardwood plywood for interior uses (Ejiogu *et al*., 2018). Due to its low price, good technological properties, absence of colours in cured polymer and easiness of application for a variety of curing conditions, Urea formaldehyde resin is one of the most preferred adhesives in wood composite board production (Boran *et al*., 2011). Over many years, excellent formulations have been developed for wood application. Although some trial and error industrial research has been and is still on in the field of resin formulations. However, resin knowledge has progressed to such an extent that scientific principles are used today to develop resins of ever improving performance (Nuryawan *et al*., 2014).

For many years, nano materials have received much interest for application in adhesives because nanoparticles could be beneficial in the development of more moisture-resistant UF adhesives, this has led to a rise in the application of nanotechnology in the wood industry (Bardak *et al*., 2018). Not much investigations have studied chemical modifications of the adhesive formulation, this may be because any modification of urea formaldehyde resin must be of low cost and also allows the adhesive to be processed by using conditions (equipment, cure time and temperature) that are similar to those used with neat urea formaldehyde or the modifications will not be practical (Rachtanapun and Heiden, 2002).

Particleboard application segment dominates the global Urea formaldehyde resin market with a market share of approximately 35 % (Lubis *et al*., 2018). This huge share of particleboard segment can be attributed to growing number of housing projects across the globe as a result of growing population coupled with rising economies.

Bharath and Swamy (2009) stated that the increasing interest in introducing degradable, renewable and inexpensive reinforcement materials which are environmental friendly has stimulated the use of hard cellulose biomass. The low cost, less weight and abundant availability make the natural fibres an attractive alternative for Urea formaldehyde resin modification. Producing Nano materials with unique properties is expected to revolutionize material engineering technology and confer some special qualities to the new material. According to Park and Causin (2013), Nano science and nanotechnology also has numerous advantages for wood composite materials. In spite of the advantages of Urea formaldehyde resin over other adhesives, they possess some disadvantages mainly; lower resistance of urea formaldehyde to water which limits the use of wood based panels bonded with Urea formaldehyde resin adhesives to interior applications and formaldehyde emissions resulting primarily from Urea formaldehyde resins in wood based composite panels.

The use of nanotechnology in the manufacture of particleboard and plywood panels is of great importance to overcome the formaldehyde emission challenges when used with the proper nanomaterial type and loading level as stated by Candan and Akbulut (2013). Roumeli, (2011) pointed out that technology offers the possibility of using additives with dimensions in the Nano scale. Such materials seem promising because Nano particles have large surface area and can bring on new properties of the resin that they are impregnated with.

Candan and Akbulut (2013) again studied the development of environmentally friendly wood composite panels by nanotechnology, Urea-formaldehyde and melamine urea formaldehyde resins were reinforced with various nanomaterials at different loading levels. The result obtained from this work indicated that nanomaterial reinforcement with Nano $SiO_2$, $Al_2O_3$ and ZnO decreased formaldehyde emissions of the composite panels at proper loading levels.

Matykiewicz (2020) work titled biochar as an effective filler of carbon fiber reinforced bio-epoxy composites showed that biochar produced from willows was successfully used as a low-cost filler in carbon fiber-reinforced epoxy composites. Due to its specific properties, the introduction of biochar to the epoxy matrix contributed to the improvement of the thermomechanical properties of materials, such as storage modulus, and mechanical properties, such as flexural and impact strength. Also, biochar has functional groups on its surfaces which facilitate its interaction with the polymer matrix.

Bardak *et al.* (2018) reported that nanoparticle modified Urea-formaldehyde resin adhesive showed better bonding strength as against pure UF resin. Nano silicon dioxide ($SiO_2$) and titanium dioxide ($TiO_2$) were blended with UF. The addition of nano-$SiO_2$ and nano-$TiO_2$ drastically changed the physicochemical properties of UF adhesive when examined under an X-ray diffraction machine.

Roumeli *et al.* (2011) studied the synthesis, characterization and thermal analysis of Urea-formaldehyde/nano$SiO_2$ resins, UF resins containing different quantity of $SiO_2$ nanoparticles were studied and the results showed that silanol groups of $SiO_2$ interacted with UF resin to form hydrogen bonds, aggregates of $SiO_2$ nanoparticles were formed in UF resin and their size increases as $SiO_2$ content is increased. The curing reactions were examined with Differential Scanning Calorimetry (DSC) and it was revealed that curing

temperature of UF resin was slightly affected by the addition of nanoparticles. Thermogravimetric analysis (TGA) also revealed that $SiO_2$ nanoparticles did not have an effect in the thermal stability of the resin.

## 1.2 Statement of the Research Problem

Particleboard bonded with unmodified Urea formaldehyde resin lack water resistance, this is due to the low stability of the amino-methylene bond making it susceptible to hydrolysis and thus making it have limited application. This has limited the use of particleboard bonded with unmodified Urea formaldehyde resin to mostly interiors only (Bardak *et al.,* 2018). With the ever increasing demand for wood and wood based products for both interior and exterior use, there is the need to improve the hydrophilic property of unmodified UF resin so as to remove its limitation while ensuring the properties of the modified resins are similar to those of the unmodified resins (Rachtanapun and Heiden, 2002). In other to obtain a more water resistant urea formaldehyde resin, additives which include organic and inorganic materials are extensively used in resin formulation.

## 1.3 Aim and Objectives of the Study

The aim of this study is to modify Urea formaldehyde resin adhesive using nanoparticles derived from bamboo waste and its application in particleboard production. This aim will be achieved through the following objectives :

i. Preparation and characterization of biochar and nano biochar produced from waste bamboo.
ii. Synthesis and characterization of neat and modified UF resin using Alkaline-Acid method.

iii. Production and characterization of particleboards using the neat and modified adhesives.

## 1.4 Justification of the Study

Nanomaterial bonded resins have a modifying effect on the resins and improves its physical and mechanical properties. Available literatures have shown that urea formaldehyde resin modified with nanoparticles of both organic and inorganic materials become less hydrophilic after modifications.

## 1.5 Scope of the Study

This study will be limited to the development of Nano particles from bamboo biochar, modification of Urea-formaldehyde resin with the produced nanoparticles and application of the modified urea formaldehyde resin in particleboard production.

# CHAPTER TWO

# 2.0 LITERATURE REVIEW

## 2.1 Adhesives

Adhesives are materials that are used to glue two pieces of substrates together, the substrates can either be of the same kind or of two different types and the cause of adhesion can be both chemical and physical according to Joakim, (2012). Chemical adhesion is when the adhesive and the substrate interact chemically to form covalent bonds between them. Physical adhesion occurs when the substrates undergo mechanical interactions or secondary forces such as; dipol-dipol interaction, hydrogen bonds, electrostatic interactions or van der waal forces. Adhesives have an important place in wood industry. The quality and durability of a wooden product primarily depend on the quality of its adhesive bonding. Many difficulties in applying wood as an engineering material arise from variations in moisture content. This situation also has a negative effect on the adhesive performance (Bardak *et al.,* 2018). Adhesives may be applied in a variety of ways depending on the form it comes in. Adhesives may be spread on a surface manually, or may be dispensed using a variety of sophisticated nozzles and robotic equipment that is currently available. Maintaining adherent cleanliness and providing adequate cure conditions may all be important considerations for certain types of adhesives.

## 2.2 Properties of Adhesives

### 2.2.1 Viscosity

Rheological properties such as the viscosity and the dynamic modulus can be directly correlated to the evolving physical and mechanical properties during resin cure. Viscosity of a paint binder affects flow properties such as leveling and sagging (Osemeahon *et al*., 2007). Film forming property, adhesion property and drying rate of paint film are also functions of viscosity.

### 2.2.2 Gelation time

The gel time is one of the most important kinetic characteristics of curing, because it describes the attainment of certain critical conversion responsible for the transition from liquid to solid state of the curing process However, the need for short or long gelation time varies for different adhesives depending on their specific need. The gelation time is apart from composition and structure of the resin also dependent on the hardener and amount of hardener being used as well as the curing temperature (Joakim, 2012). The result of this test does not just include the time during which the resin gels. Important further information may be obtained such as whether the resin gels sharply within 1 or 2 s, or whether its gel point spans 10 s or more, the latter case forecasts a slow generation of cohesion bonding strength.

### 2.2.3 Density

The density of a paint binder has a profound influence on factors such as pigment dispersion, brushability of paint, leveling and sagging. Density depends on free volume and packing efficiency of molecular chains, the reduction in density with increase in molecular weight indicates inefficient molecular packing (Osemeahon *et al*., 2007).

## 2.3. Applications of Adhesives

Adhesives are designed for specific applications and besides their role in the adhesion process, they can be used for other purposes such as sealing agents, in order to eliminate the effect of self-loosening caused by dynamic loads, sealing of areas to prevent oxidation and corrosion. Sealants can be used as electrical or thermal insulators, fire barriers and products for smoothing, filleting or flying. The materials that are used as sealants have lower Strength than those used as adhesives, because sealant formulations contain large amounts of inert filler material for cost reduction and gap filling purposes. Certain sealants, like adhesives, can be used to assemble parts, and many adhesives can be used to seal. Dinte and Sylvester (2018) stated that the adhesives and sealants are mainly used to bond the following substrates: metals, plastics (thermosets and thermoplastics), composites, foams, elastomers, wood and wood products, glass and ceramics and sandwich and honeycomb structures. The main areas of adhesives applications are as follows;

i. Construction: floor tile and continuous flooring installation, ceramic tile installation, countertop lamination, manufacture of prefabricated beams and trusses, carpet adhesives, flooring underlayment adhesives, installation of prefinished panels, joint cements, drywall lamination adhesives and covering installations (Ormondroyd, 2015).
ii. Biomedical and pharmaceuticals: Various medical adhesive tapes/dressings/devices are used to cover and protect wounds, to seal the skin edges of a wound or to support an injured part of the body. Advanced adhesives have a wide range of biomedical and pharmaceutical applications and are currently used in various medical procedures, as medical devices: restorative dental filings, blood transfusions, anaesthetic administration, intravenous drug

delivery, heart bypass surgery, urological surgery and plastic surgery (Pal *et al*., 2011).

iii. Consumer adhesives: model and hobby supplies, decorative films, school and stationery products.

iv. Packaging: carton-side seam and closures, composite bonding of disposable products, bags, labels, cups, cigarette and filter manufacture, specialty packages (cosmetics, toiletries), composite containers and tubes (Ouarhim *et al*., 2019).

v. Tapes: packaging, industrial, surgical, masking, and consumer tapes.

vi. Transportation: auto, truck and bus assemblies, weatherstrip and gasket bonding, aircraft and aerospace structural assemblies.

vii. Other rigid bonding: shake-proof fastening; furniture manufacture; manufacture of millwork, doors, kitchen cabinets and vanitories; appliance assembly and trim attachment; TV, radio and electronics assembly and machinery manufacture and assembly.

viii. Other non-rigid bonding: apparel laminates, shoe assembly, sports equipment, book binding, rug backing, flock cements, air and liquid filter manufacture (Ormondroyd, 2015).

## 2.4 Resins

Resins are chemical compounds or viscous substances that convert into rigid polymers through a curing process. Resins are naturally occurring but are now often made synthetically. Some synthetic resins have similar properties to natural plant resins, but many are very different. Resins can be derived from polymers, monomers, oils, fatty acids and natural sources (Sun *et al*., 2014).

### 2.4.1 Types of resins

#### 2.4.1.1 *Thermoplastic resins*

Thermoplastic resins are substance that softens when heated and when cooled, it hardens again. These resins can further be classified into the following;

i. Alkyd resins

These are made by heating polyhydric alcohol with polybasic acids. They possess great electrical and thermal properties along with it a good chemical resistance. Quite cost effective and used for electric components, paints and putty filers (Hisham *et al*., 2011).

ii. Polycarbonate resins

These are generally made from Bisphenol A and phosgene. Due to their inherent advantages, they are used for metal replacements, lenses, safety helmets, insulators and photography film (Hisham *et al*., 2011).

iii. Polypropylene resins

These are a type of thermoplastic polymer resin that does not contain Bisphenol A. They are colorless, tasteless with a great heat resistance and low density. They also possess a great chemical resistance and are used for toys, pipe and production and coatings (Yong No and Kim, 2004).

#### 2.4.1.2 *Thermosetting resins*

Thermosetting resins are substances (typically synthetic resins) that set permanently when heated. They are usually in the soft solid or viscous state on heating and undergoes extensive cross-linking in moulds and become irreversibly hard as well as

insoluble products (Ouarhim *et al*., 2019). Thermosetting resins can be further classified into the following;

Phenolic resins

They are one of the types of thermosetting resins and possess a strong heat and impact resistance to chemical corrosion and moisture penetration. They are used for a variety of products like brake linings, electrical components, moulds, adhesive for cements (Kandelbauer *et al*., 2007).

Polyester resins

They are formed by the reaction of polyhydric alcohols and dibasic organic acids. The best thing about it is they have quite an excellent resistance to heat and chemicals. They are quite cost effective and are extensively used for construction, fishing rods, decorative accessories, coatings and in plane and ship components (Hisham *et al*., 2011).

Epoxy resins

They are a type of reactive prepolymers and polymers belonging to the epoxide group. They have an excellent chemical and heat resistance and great adhesive properties, used extensively in laminates, linings, propellers and surface coatings (Bartoli *et al*., 2019).

**2.5 Urea Formaldehyde**

Urea formaldehyde resin is an adhesive formed by the reaction of Urea and Formaldehyde. It consists of $[(O)CNHCH_2NH]_n$ repeat units (Nuryawan *et al*., 2014). Plate I shows the structures of urea and formaldehyde. Urea, also known as carbamide is an organic compound with chemical formula $CO(NH_2)_2$. This amide has two $NH_2$

groups joined by a carbonyl functional group (Park and Jeong, 2011)[a]. It is a colourless, odourless solid, highly soluble in water and practically nontoxic. Formaldehyde is a naturally occurring organic compound with the formula $CH_2O$. It is the simplest of the aldehydes (R-CHO) (Ejiogu *et al*., 2018).


**Plate I**: Structures of Urea and Formaldehyde (Peep *et al*., 2006)

The chemistry of the reaction of Urea-formaldehyde resin takes place in two stages as stated by Patel and Amin (2013). In the first stage, urea is hydroxymethylolated by the addition of formaldehyde to the amino groups. This reaction in reality is a series of reactions that lead to the formation of mono, di and trimethylolureas (Park and Jeong, 2011)[b]. The addition of formaldehyde to urea takes place over the entire pH range. The reaction rate is dependent on the pH (Singh *et al*., 2014). The second stage of urea-formaldehyde resin synthesis consists of the condensation reaction of the methylol ureas to low molecular weight polymers. Joakim (2012) noted that the rate at which these condensation reactions occur is very dependent on the pH and for all practical purposes, occurs only at acidic pH. The stages of urea formaldehyde formation are shown in Plate II.

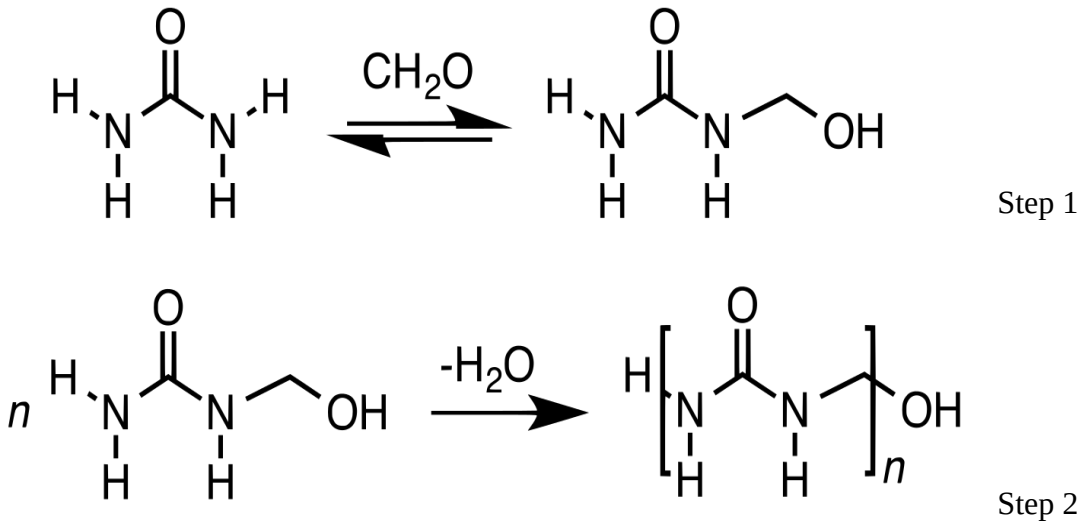


**Plate II**: Urea formaldehyde formation (Ohalete and Popoola, 2015)

**2.6 Composites**

Nagavally (2016) described a typical composite material as a system of materials composing of two or more materials (mixed and bonded) on a macroscopic scale. Composite materials are materials made from two or more than two materials with considerably differ in physical and chemical properties, that when combined, make a material with appearances different from the individual components. One material is the binder or matrix and the other material is known as the reinforcement. The matrix binds fibres or fragments of the reinforcement (Ezeribe *et al*., 2014). Composites comprise strong load carrying material is known as reinforcement and weaker materials is known as matrix. Reinforcement provides stiffness and strength which helps to support structural load. Composite materials do not lose their respective identities but still relate their properties to the product causing from their mixture (Gupta *et al*., 2016). Composites have many benefits with respect to their selection and use. The selection of the materials depends on the performance and intended use of the product. Nowadays

Composite technology is applied to a growing variety of functions from lightweight fishing poles to automobile or aircraft, and from machine tool bits to the thermal protection systems for space reentry vehicles. The expanding activity in composites is stimulated both by the demands of such applications and by the potential embodied in the outstanding properties which have been achieved in substances such as high strength glass filaments or stiff refractory graphite filaments. They are used as reinforcing materials in the fiber reinforced plastics which have been widely accepted as materials for structural and non-structural applications according to Bharath and Swamy (2009). Some benefits of composites include the following;

Light weight

High strength-to-weight ratio

Corrosion resistance

Dimensional stability

Low thermal conductivity

High impact strength

Low maintenance

Long term durability

Tailored surface finish

**2.7 Particleboard**

Particleboard shown in Plate VI is a panel product manufactured from lignocellulosic materials, primarily in the form of discrete particles, combined with a synthetic resin or

other suitable binder and bonded together under heat and pressure. The demand of composite wood products such as particleboard, plywood, hardboard, oriented standard board, medium density fiberboard and veneer board has hiked significantly throughout the world. Among them, the demand for particleboard has been increasing significantly because of house construction, interior decoration, manufacturing of furniture flooring, home constructions, countertops, stair treads, cabinets, tabletops, vanities, speakers, sliding doors, lock blocks, interior signs, displays, table tennis, pool tables, electronic game consoles, kitchen work tops, and work surfaces in offices, educational establishments, laboratories and other industrial products (Wahab *et al*., 2018). This huge demand for particleboard accelerates the declining rate of natural forest resources. Consequently, it has raised a vital issue of the continuous supply of raw material to the wood based sectors. Thus, the demand of alternative sources of raw materials is increasing ever more. Alternate lignocellulosic materials like agricultural residues and non-woody plant fibers may play a major role in minimizing the demand of manufacturing the composite panels (Alam *et al.,* 2015).

There are two major processes of making particleboard

Flat–pressed boards: Pressing the boards flatwise in single or multiple-opening hot presses.

Extruded boards: continuously extruding the boards through a hot extrusion die.

**Plate III**: Saw dust for particleboard production

Today, manufacturing agglomerated materials, including particleboards, is based on the idea of utilizing the wood waste of lower value resulting from wood processing, such as sawdust shown in Plate III, chips, particles, and wood pulp. An increase in the volume of particle board manufacturing has resulted in manufacturers seeking new material resources. At the present time, besides natural wood, other lignocellulose materials, as well as recycled wood, are used, especially in countries where there is a scarcity of wood resources (Izdinsky *et al*., 2020). The particleboard industry uses mostly wood shavings from saw mills, resulting in a higher quality product due to better control of the homogeneity of raw material. Apart from residues, the raw materials found in large amount at regional level can decrease the final cost of the product (Melo *et al.*, 2014). The presses used to manufacture moulded particleboard products are press moulds equipped with a heated die that shapes the resinated wood particles into the finished product. Press temperatures can range from 132 °C to 288 °C. Press temperature and time vary according to the moulded product being produced. After pressing, the boards

generally are cooled prior to stacking. The particleboard panels then are sanded and trimmed to final dimensions.

**Plate IV**: Metal mould plate

The following sequence of operations applies to the production of particle boards as stated by (Abdellaoui *et al*., 2019);

i. Hogging, grinding, hammer milling or machining the wood raw material to the desired particle size and shape.
ii. Drying the particles to uniform, predetermined moisture content, and in some cases, screening out the fines.
iii. Adding controlled amounts of binder and other additives by spraying or other means, mixing the ingredients thoroughly. At the present time, urea resins are the most common binder, although the use of phenol resins is growing.
iv. Flat pressing or extruding the boards under controlled heat and pressure to a density about 20 to 30 percent greater than that of the species in the particles.
v. Cooling, trimming, and equalizing the moisture content in the formed boards.


**Plate V**: Compression mould machine

Plates IV and V show a metal mould plate and compression mould machine used in the pressing and formation of particleboard.

**Plate VI**: Typical pictures of Particleboards (Dinte and Sylvester, 2018)

### 2.7.1 Properties of particleboard

#### 2.7.1.1 *Density*

The density value of a composite material system is an important property which determines its performance in service environment (Dotun *et al*., 2018). Particleboards are grouped into low density, medium density and high density particleboards. Composite with low density tend to have high porosity. This low density is why water

quickly enters the pores of particleboard so that the water will break the bond between filler, fiber, and matrix.

#### 2.7.1.2 *Water absorption*

The interaction of structural network of polymer resins with water is both of fundamental and technical interest, water absorption affects vital properties of the polymer material such as the physical, mechanical, thermal and structural properties. One of the major drawbacks of UF resin is poor water resistance, water absorption in polymer network is related to the availability of molecular size holes in the polymer structure and the polymer water affinity (Dotun *et al*., 2018).

#### 2.7.1.3 *Thickness swelling*

Thickness swelling testing is carried out to determine the performance of the particleboard when in contact with water. Usually, the particle board exposed to water will expand due to the release of bonds between the composite components. It is known that the particle board on the market is very quickly damaged or destroyed when exposed to water. Thickness swelling is a physical property that can be seen directly. The particleboard, when in contact with water, will cause dimensional changes. Thickness swelling is strongly influenced by filler type characteristics, the higher percentage of thickness swelling, the worse particleboard performance (Lusiani *et al*., 2020).

#### 2.7.1.4 *Hardness*

Hardness testing is carried out to determine how strong the particleboard is when other materials scratch it. Because in its application, particleboard will come into contact with other objects. The hardness testing is done by the ball indentation method or equal to

Rockwell hardness type H. The value acquired is called ball indentation hardness ($N/mm^2$). This surface hardness correlates directly with porosity formed during the manufacturing process. The filler distribution pattern in the composite will affect the mechanical properties of the particleboard. The homogeneous distribution of fillers can provide higher hardness and strength than the distribution of fillers that are not uniformly and lumpy. This filler distribution can be studied from hardness at any point in the material surface. If the hardness at any point has the same value, it is said that filler distribution is uniform (Lusiani *et al*., 2020)

#### 2.7.1.5 *Impact toughness*

Impact tests are carried out to determine the particleboard's toughness when it falls, or there is a collision with another object. Impact strength of particleboard is greatly influenced by the particle size, fibre distribution, particle orientation and particle-polymer adhesion (Chiang *et al*., 2016).

#### 2.7.1.6 *Tensile properties*

Tensile testing is a form of tension testing and is a destructive engineering and material science test whereby controlled tension is applied to a sample until it fully fails (Wahab *et al*., 2018). The ultimate tensile strength is the maximum stress that a specimen is exposed to during testing. This may differ from the specimen’s strength when breaking depending on if it is brittle, ductile or has properties of both (Nurdin *et al*., 2018).

The modulus of elasticity also known as Young’s modulus measures the stiffness of a specimen whereby the material will return to its original condition once the load has been removed (Wahab *et al*., 2018).

Elongation at break determines to what extent a material stretches before breaking and hence the ductility or flexibility of the material. One of the shortcomings of UF resin is that it is too hard and brittle and hence poor resistance to crack propagation. Particleboard must be able to withstand stresses emanating from variation in environmental factors. Therefore, in developing adhesives from amino resins, tensile property such as elongation at break must be taken into consideration (Lusiani *et al*., 2020).

## 2.8 Biomass

Biomasses in simple terms are organic materials that are not synthetic or manmade sourced from plants or animals (Mohammad *et al.,* 2015). Recently, with running out of the natural sources and increasing environmental awareness, biomass has gained significant interest as a reinforcing material instead of inorganic reinforcements such as glass fibers. In addition to environmental benefits, owing to low prices and steadily rising performance of technical and standard plastics. Besides, biomass offer some advantages such as high specific modulus, high specific strength, low density, availability of renewable natural resources, and biodegradability (Bodur *et al.,* 2016).

One of the issues of biomass is the scattered information and the differences in mechanical properties reported. Also, the lack of standards for both producers and users of these materials regarding methods to collect, treat, process and post-process biomass adds to the complexity of selection. These issues are in fact critical for generalized use of biomass in different applications (Pecas *et al*., 2018).

Biomass consists of lignin, cellulose, and hemicelluloses. Lignin and hemicelluloses are amorphous in structure while cellulose is semicrystalline and thus, differs in its physical and mechanical properties (Mahardika *et al.,* 2018). The specific mechanical properties

of biomass are comparable to those of traditional reinforcements. Thus, the essential properties of biomass can satisfy the requests of the global market especially for those industries concerned in weight reduction. That is why they can be potential substitute for non-renewable synthetic materials. However, high moisture absorption, poor wettability and insufficient adhesion between biomass and polymer matrix lead to debonding at fibre-matrix interface (Biswas *et al.,* 2015).

## 2.9 Bamboo

Bamboo is a strong, fast growing and very sustainable material and have been receiving interest because it has a high strength to weight ratio, one of the fastest growing plants, requires less water, no use of pesticides or herbicides and is harvested at its base, leaving the root intact (Kaminski *et al.*, 2016). Also, the fibre surface is round and smooth. It is light, stiffer and stronger than glass fibre (Pecas *et al.,* 2018). Bamboo has provided abundant and high-quality cellulose fibres for centuries, becoming a primary feedstock for weaving, pulp, paper, and fiber-based composite industries. The main chemical compositions of bamboo include cellulose, hemicellulose, and lignin, all kinds of extractions, a little ash, and silicon dioxide. All of these structures and characteristics contribute to bamboo's superior strength, toughness, bending ductility, and low density as reported by Wang and Chen (2017). Bamboo, as a kind of wood, is mainly composed of hemicelluloses, cellulose and lignin that can produce higher value-added products by pyrolysis processes. Furthermore, it possesses many other advantages such as easy propagation, fast growth and low ash content (Mena *et al.,* 2014). Bamboo stems are shown in Plate VII.

**Plate VII**: Bamboo stems (VanDam *et al.,* 2018)

### 2.9.1 Uses of bamboo

VanDam *et al*. (2018) broadly categorized the uses of bamboo according to commercial application, these are as follows:

i. Horticultural support sticks
ii. Plaiting
iii. Tools and utensils (including chopsticks and toothpicks)
iv. Scaffolding
v. Construction and composite materials (flooring, plywood, veneer, and laminated bamboo)
vi. Furniture, furnishings

vii. Pulp, paper, and boards

viii. Textiles and tissues

ix. Handicrafts, musical instruments, and gift items

x. Food and feed products (shoots, dietary fiber, tea leaves, and beverages)

xi. Energy (combustion) and charcoal.

## 2.10 Biochar

Biochar is a fine grained product of carbonization, characterized by a high content of organic carbon and low susceptibility to degradation, which is obtained through the pyrolysis of biomass and biodegradable wastes (Saletnik *et al.*, 2019). Biochar is a carbon-rich solid derived from the pyrolysis of biomass with little or no oxygen (Ghyselsa *et al*., 2019). Biochar is usually produced from crop residues, wood biomass, animal litters and solid wastes through various thermochemical processes, including slow pyrolysis, fast pyrolysis, hydrothermal carbonization, flash carbonization, torrefaction and gasification (Tan *et al.*, 2016). Biochar originating from biomass is typically 20-40 % of dry lignocellulose biomass (Patryk *et al*., 2016). However, the yield and chemical properties of the pyrolysis products are strongly influenced by operating conditions during pyrolysis such as temperature, heating rate, holding times, particle size, atmosphere and feedstock (Liu *et al*., 2018). Depending on the final use of biochar, the required properties of the material may be different (Mena *et al.*, 2014). Plate VIII shows a picture of biochar produced from the pyrolysis of biomass.

**Plate VIII**: Typical picture of Biochar (Mary *et al*., 2016)

## 2.11 Pyrolysis

Pyrolysis is a thermochemical decomposition process that takes place in the absence of oxygen to produce a liquid phase (tar or hydrocarbon liquids and water), a carbon rich solid phase (charcoal) and non-condensable gases ($CH_4$, $CO_2$, CO, $H_2$,), (Mena *et al*., 2014).

Pyrolysis as a thermo-chemical conversion of biomass is one of the many technologies that can convert biomass into valuable products and is an efficient means with less emission to produce alternative fuels from biomass (Oyedun *et al*., 2012).

### 2.11.1 Basic principle of pyrolysis

The thermal decomposition process of pyrolysis using lignocellulosic biomass takes place in the absence of oxygen under inert atmosphere. As an inert atmosphere argon or nitrogen gas flow is usually needed. The fundamental chemical reaction is very complex and consists of several steps (Phuakpunk *et al*., 2020). The end products of biomass pyrolysis consist of biochar, bio-oil and gases. Pyrolysis process emits mainly methane, hydrogen, carbon monoxide and carbon dioxide. The organic materials present in the biomass substrate starts to decompose around 350–550°C and it can proceed until 700–800°C without the presence of air/oxygen (Suman and Gautam, 2017). Biomass is mainly composed of long polymeric chain of cellulose, lignin, hemicellulose, pectin and others. The larger molecules of organic materials start to decompose to yield smaller molecules, which are released from the process stream as gases, condensable vapours (tars and oils) and solid char during pyrolysis process. The proportion of each end product depends on the temperature, time, heating rate, and pressure, types of precursors and reactor design and configuration (Zaman *et al*., 2017).

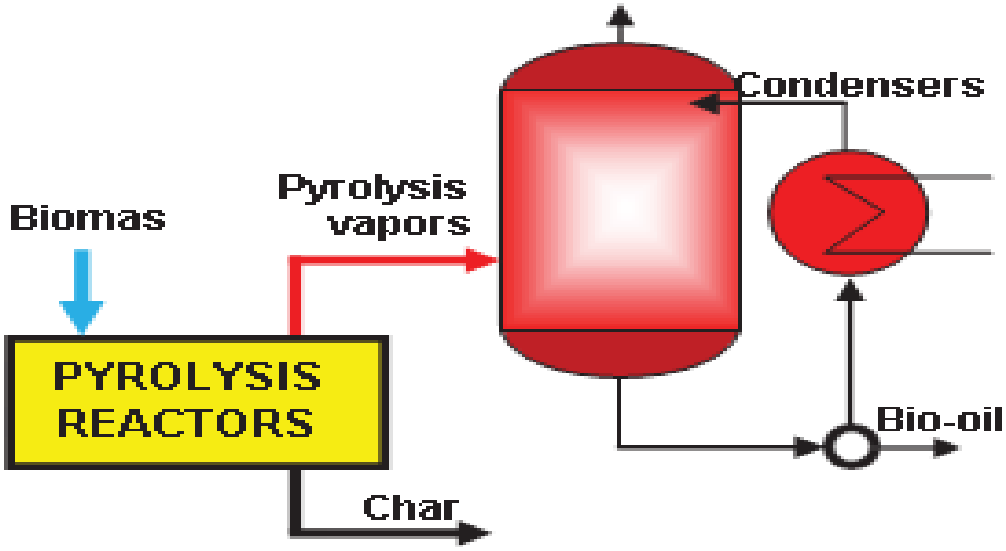


**Plate IX**: Flow diagram of a typical pyrolysis unit (Zaman *et al*., 2017)

Plate IX shows a flow diagram of a typical pyrolysis unit and the products formed.

### 2.11.2 Types of pyrolysis

Pyrolysis are classified into different types depending on the parameters applied (temperature, heating rate, residence time and pressure) and quantity of products formed from the reactor (Saletnik *et al*., 2019).

#### 2.11.2.1 *Slow pyrolysis*

In slow pyrolysis process, the time of heating the biomass substrate to pyrolysis temperature is longer than the time of retention of the substrate at characteristic pyrolysis reaction temperature. The residence time of vapour in the pyrolysis medium is longer for slow pyrolysis process. This process is mainly used to produce char. It can be further classified as Carbonization and Conventional. (Zaman *et al.*, 2017)

#### 2.11.2.2 *Fast pyrolysis*

During the fast pyrolysis process, biomass residues are heated in the absence of oxygen at high temperature using higher heating rate. Based on the initial weight of the biomass, fast pyrolysis can provide 60–75 % of liquid biofuels with 15–25 % of biochar residues.

#### 2.11.2.3 *Flash pyrolysis*

This procedure is carried out by speedy devolatilization under inert atmosphere using higher heating rate with high pyrolysis temperatures around 450 and 1000°C. The flash pyrolysis process of biomass can give solid, liquid and gaseous products. The bio-oil production can go up to 75% using flash pyrolysis (Wild, 2015).

Table 2.1 shows a summary of the various types of pyrolysis, the conditions at which they depend on and the products formed.

**Table 2.1: Types of pyrolysis**

| Pyrolysis | Conditions | Liquid | Solid | Gas |
|---|---|---|---|---|
| Slow-Torrefaction | Reaction temperature~290 $^{o}$C, heating rate up to 1 $^{o}$C/sec, solid residence time ~ 30 min. | 0.5 % | 72-77 % solid | 23 % |
| Slow-Carbonization | Reactor temp. 400-500 $^{o}$C, heating rate up to 1 $^{o}$C/sec. long solid residence hrs.-days. | 32 % | 33 % Char | 35 % |
| Intermediate | Reactor temp. 400-500 $^{o}$C, heating rate range 1-1000 $^{o}$C/sec, hot vapour residence~10-30 s | 50 % | 25 % Char | 25 % |
| Fast | Reactor temperature 500 $^{o}$C, very high heating rates >1000 $^{o}$C/sec short vapour residence ~ 1 s | 75 % | 12 % Char | 13 % |

(Wild, 2015)

## 2.12 Nanotechnology

Nanotechnology is the science of the small; the very small. It is the use and manipulation of matter at a tiny scale. At this size, atoms and molecules work differently, and provide a variety of surprising and interesting uses (Pal *et al.*, 2011). The nano sized world is typically measured in nanometers (1nm corresponding to $10^{-9}$ m) and it encompasses systems whose size is above molecular dimensions and below macroscopic ones (generally > 1 nm and < 100 nm). Candan and Akbulut (2013) also described nanotechnology as the manipulation of materials measuring 100 nm or less in at least one dimension. Keskinbora and Jameel, (2018) stated that nanotechnology is the next giant step in science that sets humankind in control of a wholly new dimension and enable them to manipulate the environment at molecular level.

## 2.13 Nanoparticles

Nanoparticles are generally defined as particulate matter with at least one dimension that is less than 100 nm (Khan *et al*., 2017). In recent years, nano sized fillers such as nanoparticles, nanotubes, nanoclay and nanofibers have been considered as filler materials for epoxy and protein adhesive to produce high performance composites with enhanced properties (Sadare *et al*., 2015). In recent years, nanoparticles have been synthesized largely from agricultural and industrial wastes. Post-harvest wastes form a large part of the biomass on the field and are usually burned, these waste can be used as biological sources for the green synthesis of nanoparticles. The use of these waste materials compared with the physical and chemical methods has benefits including reduction of using harmful chemicals, low-cost, low energy, and renewing waste material (Huynh *et al.,* 2020).

### 2.13.1 Synthesis of nanoparticles

Synthesis of nanoparticles as shown in plate X is broadly divided into two approaches, the bottom-up approaches and the top-down approaches.

#### 2.13.1.1 *Bottom-up approaches*

This involves chemical reduction of materials for the synthesis of nanoparticles. It is simple and gives liberty in selection of molar concentration of reactants, dispersant and the feed rate of the reactant to acquire nanoparticles with desired size, shape and size distribution. Some of these approaches include; electrochemical reduction method, photochemical method, hydrothermal approach, co-precipitation method and chemical vapour deposition method (Sajid and Plotka-Wasylka, 2020).

#### 2.13.1.2 *Top-down approaches*

Top-down approaches are characteristically simpler and rely on mechanical methods of breaking down materials to form nanoparticles. Ball milling is one of the ways of preparing nanoparticles. Advantages of this method of nanoparticles synthesis include; it is inexpensive, it involves old well established processes and particle sizes of 2-20 nm are possible. It also has some disadvantages such as irregular particles, introduction of defects and introduction of impurities from balls and milling additives.

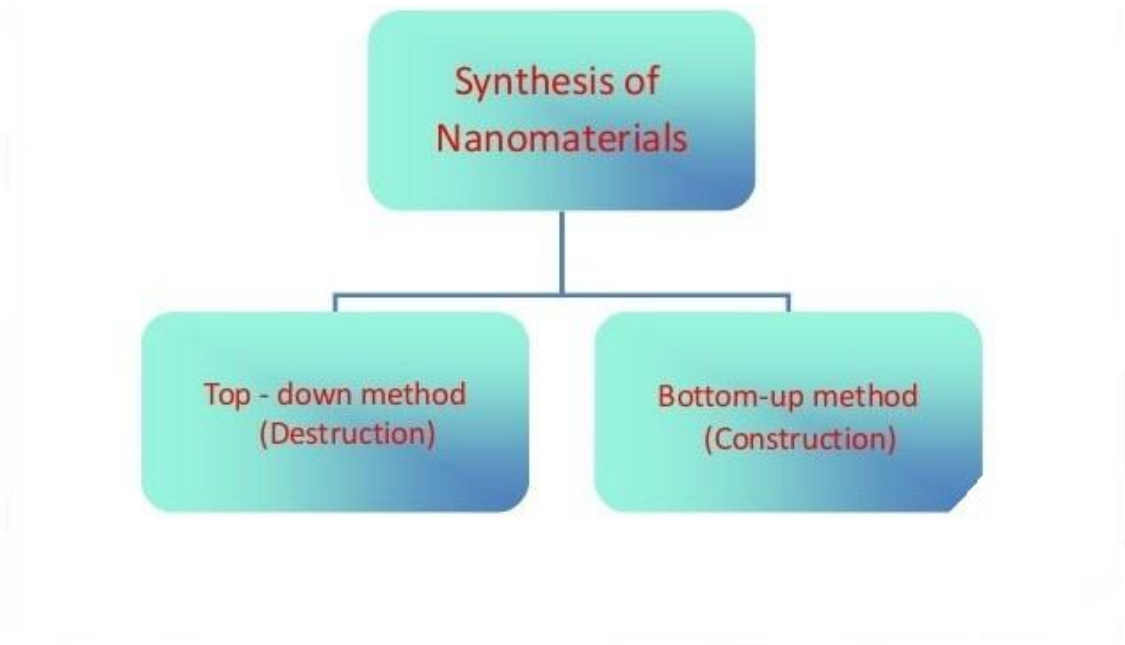


**Plate X**: Methods of Nanomaterial synthesis

### 2.14 Ball Milling (Top-down Approach)

Agrawal and Yi (2020) described ball milling as a shear-force dominant process where the particle size goes on reducing by impact and attrition mainly consists of metallic balls (generally or steel balls), acting as grinding media and rotating shell to create centrifugal force. Ball mills are a common occurrence in industry for the production of fine particles. During the ball milling process, there are two factors that contribute to the exfoliation. The main factor contributing is the shear force applied by the balls. The secondary factor is the collisions that occur during milling. Harsh collisions can potentially disrupt the crystal structure resulting in a more amorphous mass. So in order to create good-quality, high-area product, the collisions have to be minimized (Petridis *et al*., 2019).

### 2.15 Applications of Nanotechnology in the Wood Industry

The application of nanotechnology in wood industry is on the rise, nano materials have received much interest for application in adhesives due to high specific surface areas

and unique mechanical properties (Bardak *et al.*, 2018). Nano composites are formed by the dispersion of nanoparticles into the polymer. They have unique properties, such as high heat resistance, toughness and stiffness. However, studies on the assessment of nanoparticles in the adhesive industry are limited. Adhesives have an important place in wood industry. The quality and durability of a wooden product primarily depend on the quality of its adhesive bonding. Nanoparticles can help to produce enhanced wood products (Bardak *et al*., 2018). Applications of nanotechnology in the wood industry include; wood composites, pulp and paper production and production of cellulosic materials for reinforcements.

# CHAPTER THREE

## 3.0 RESEARCH METHODOLOGY

This chapter shows a list of materials and equipment used in carrying out the experiments and also the methodology used for each experiment.

### 3.1 Materials and Equipment

Table 3.1 shows a list of the materials used for biochar production, UF resin synthesis and particle board formation.

**Table 3.1: Materials used for the experiment**

| Materials | Source |
|---|---|
| Urea | NILEST Zaria |
| Formaldehyde solution | NILEST Zaria |
| Sodium hydroxide | Chem. Engineering dept. FUT Minna |
| Ammonium hydroxide | Chem. Engineering dept. FUT Minna |
| Sulphuric acid | Chem. Engineering dept. FUT Minna |
| Distilled water | Chem. Engineering dept. FUT Minna |
| Nitrogen gas | Chem. Engineering dept. FUT Minna |
| Bamboo | Gidan Kwano, Minna |
| Mahogany Saw dust | Zaria |

Table 3.2 shows a list of equipment used in carrying out all experiments in the production of nano biochar modified UF resin particle boards.

**Table 3.2: Equipment used for the experiment**

| Equipment | Specification | Source |
|---|---|---|
| TGA analyzer | PerkinElmer TGA 4000 | STEP B FUT Minna |
| Malvern instrument | Model ZEN1600 | STEP B FUT Minna |
| FTIR machine | Agilent technology CARY 630 | ABU Zaria |
| Electronic Universal Testing machine | Model WDW-100KN | ABU Zaria |
| Microvickers Hardness Tester | Model MV1-PC 07/2012-1329 | ABU Zaria |
| Charpy impact testing machine | Model 412-07-15269C HD9 6QD | ABU Zaria |
| Pyrolysis reactor | Locally fabricated | Chem. Engineering department, FUT Minna |
| Thomas-Wiley Laboratory mill | Model 4 | NILEST Zaria |
| Compression mould machine | | NILEST Zaria |
| Ball mill | | Kaduna Polytechnic |
| Furnace | | FUT Minna |
| Oven | | FUT Minna |
| Magnetic Stirrer | | NILEST Zaria |
| Heating mantle | | NILEST Zaria |
| pH meter | | NILEST Zaria |

## 3.2 METHODOLOGY

### 3.2.1 Sample collection and preparation

Bamboo was collected from a building site in Minna, Niger state. The sample was washed thoroughly with running water and then with distilled water to remove impurities. The sample was dried in an electric oven at 100 $^{o}$C for 24 h to reduce moisture content. Dried Bamboo samples were cut into smaller sizes of length 6-8 cm using a club hammer, this was then crushed into smaller sizes of length 8-10 mm using a grinding machine.

### 3.2.2 TGA of bamboo

The TGA of raw bamboo was carried out using a PerkinElmer TGA 4000 thermogravimetric analyzer and at a heating rate of 10 $^{o}$C/min to determine the stability temperatures of bamboo during pyrolysis and to determine the temperatures of transitions and reactions of the raw bamboo.

### 3.2.3 Pyrolysis of bamboo

Bamboo sample weighing 25 g was poured into a crucible and charged into the pyrolysis reactor. The air-lock was closed to avoid the introduction of oxygen. A gas cylinder containing nitrogen gas was then connected to the pyrolysis reactor and the valve opened with gas flow rate set at 1 cm/min. The power source was switched on and the desired pyrolysis temperatures of 400 $^{o}$C, 450 $^{o}$C and 500 $^{o}$C respectively were set and the bamboo allowed to undergo pyrolysis. The char was then removed from the reactor, air-cooled and kept for further analysis (Ahmed *et al.*, 2020).

### 3.2.4 Physicochemical analysis

The physical and chemical properties of the biochar were determined via proximate and ultimate analysis. The proximate analysis was determined using the standard as set by the Association of Analytical Chemistry (AOAC), 1994.

### 3.2.5 Proximate analysis

#### 3.2.5.1 *Moisture content*

Biochar sample weighing 1 g was placed in a clean, dry petri-dish and dried in an oven at 100 $^{o}$C for 120 min. The sample was then cooled in a desiccator for 30 min and the weight of the sample before and after heating was determined. The percentage moisture content was calculated using the Equation 3.1

$$\text{Moisture content} = \frac{(W1-W2)}{W1} * 100 \quad (3.1)$$

Where:

W1=Weight of sample before drying (g)

W2= Weight of sample after drying (g)

#### 3.2.5.2 *Ash content*

Biochar of mass 1 g was weighed in a crucible and put in a furnace at a temperature of 550 $^{o}$C for 30 min. The sample was allowed to cool in a desiccator and after cooling, it was weighed. The ash content was calculated using the Equation 3.2

$$\text{Ash content} = \frac{W1}{W2} \quad (3.2)$$

Where:

W1= Weight of ash

W2= Weight of dry sample

### 3.2.5.3 *Volatile matter*

Biochar weighing 1 g was poured in a crucible and put in a furnace at a temperature of 450 $^{o}$C for 10 min. The sample was weighed before and after drying to determine the amount of volatile matter using Equation 3.3

$$\text{Percentage Volatile content} = \frac{(W1-W2)}{W1} * 100 \quad (3.3)$$

Where:

W1= Weight of sample before drying (g)

W2= Weight of sample after drying (g)

### 3.2.5.4 *Fixed carbon content*

This was calculated using Equation 3.4

100 - (ash content + volatile matter content + moisture content) % (3.4)

### 3.2.6 Ultimate analysis

The sample (0.2 g) was digested with 3 cm$^3$ aquaregia (75 vol% hydrochloric acid and 25 vol% nitric acid) at a temperature of 100 $^{o}$C. The digest was filtered into a 250 ml volumetric flask and made up to the mark with distilled water. The mixture was stirred and filtered using whatman filter paper. The filtrate was analyzed for the elements present using Atomic Absorption Spectrophotometer Varian AA 280 (Okerulu *et al.*, 2017).

### 3.2.7 Preparation of nanoparticles

Preparation of nanoparticles of the biochar was carried out using a ball mill in order to achieve nanoparticle sizes. Biochar weighing 40 g was charged into the ball mill with biochar to ball ratio of 10:1. The milling was allowed to continue for 1 h followed by screening to remove oversized particles and impurities present.

### 3.2.8 Particle size analysis

Particle size analysis was done with a Malvern instrument model ZEN1600 with serial number MAL1084260. The prepared sample weighing 0.05 mg was diluted with distilled water, the diluted sample was allowed to dissolve in water and was filtered. The filtered sample was put in a sample holder and placed in the analysis chamber. The analysis was repeated three times to determine accurate results, the average results was then determined (Wu *et al*., 2017).

### 3.2.9 Preparation of urea formaldehyde resin

UF resin was prepared using the alkaline-acid method. 540 ml of formaldehyde solution was measured into a clean dried 1000 ml three neck round bottom flask. The pH of the formaldehyde was adjusted to 8-9 by addition of 2 ml of 20 % w/v sodium hydroxide solution and stirred. 235 g of urea was added to the mixture in a three neck round bottom flask. The mixture was placed on a heating mantle and heated at 60 $^{o}$C followed by stirring with a magnetic stirrer at 30 rpm. $H_2SO_4$ having 15 % concentration and volume 5 ml was added to bring the mixture to a pH of 2.7 and was heated further for 30 min until a viscous liquid was observed. NaOH of 20 % concentration and a volume of 9 ml was then added to adjust the pH to 7.0 and bring the polymerization to termination upon achieving a viscosity of about 150 cP. The resin was allowed to cool to a temperature of 40 $^{o}$C and 220 g of urea was added to make the Urea-Formaldehyde

ratio to be 1:1.25. The addition of 220 g of urea was to allow for complete reaction of formaldehyde. The mixture was stirred for 20 min to ensure complete dissolution of the urea (Wang *et al.*, 2017).

### 3.2.10 Modification of urea formaldehyde resin

Modification of the synthesized UF resin was done by weighing 3 g, 5 g and 7g of Nano biochar and poured into 150 ml of Urea-Formaldehyde in a 500 ml beaker. This was then mixed thoroughly using a magnetic stirrer with a stirring speed of 30 rpm until a homogenous mixture was obtained (Wang *et al*., 2017).

### 3.2.11 Production of particleboard

#### 3.2.11.1 *Particles preparation*

The mahogany wood chips were collected and oven dried at a temperature of 60 $^{o}$C for 2 h to remove the moisture content. The dried samples were then reduced to smaller sizes using a laboratory mill and then screened with a 1mm sieve to achieve a uniform size. The prepared wood particles were then used for the formation of the particleboards (Ejiogu *et al*., 2018).

#### 3.2.11.2 *Particleboard formation and pressing*

Urea-formaldehyde resin of volume 150 ml was measured into a beaker. Ammonium chloride weighing 1 g was then weighed into the Urea-Formaldehyde resin in the beaker and stirred until it dissolves completely. The wood particles were then weighed into a plastic bowl and the Urea-formaldehyde and ammonium chloride mixture poured in it followed by mixing. The mixture was then spread in a steel mould wrapped with aluminium foil which was then placed on a hydraulic pressing machine at a temperature of 160 $^{o}$C and a pressure of 2.5 MPa. It was allowed in the pressing machine for a

pressing time of 5 min. It was then removed, air-cooled and labeled accordingly for further analysis (Ejiogu *et al.*, 2018).

Tables 3.3 and 3.4 show modified resin formulation and particle board formations using neat and modified UF resins. UF1, UF2 and UF3 represents resins modified with biochars produced at 400 $^{o}$C, 450 $^{o}$C and 500 $^{o}$C respectively. 150 ml of the neat resin was modified with 3 g of biochar samples.

**Table 3.3: Resin Formulation and Modification**

| Nanobiochar Sample | Resin volume (ml) | Mass of biochar (g) |
|---|---|---|
| 400 $^{o}$C (UF1) | 150 | 3 |
| 450 $^{o}$C (UF2) | 150 | 3 |
| 500 $^{o}$C (UF3) | 150 | 3 |

**Table 3.4: Particleboard Formation**

| Wood particles (g) | UF1 | UF2 | UF3 |
|---|---|---|---|
| 40 | S1 | S2 | S3 |

Each particleboard sample S1, S2 and S3 was prepared by mixing 40 g of mahogany wood particles of size 1 mm with modified UF resins UF1, UF2 and UF3 as indicated in Tables 3.4.

### 3.2.12 Physical and mechanical properties of particleboard

#### 3.2.12.1 *Density*

The densities of particleboard samples were calculated using the British code of standards BS EN 323 which is the formula for density of a homogenous material shown in Equation 3.5

$$\rho = \frac{m}{v} \tag{3.5}$$

Where $\rho$ = Density

m = mass (g)

v = volume ($cm^3$)

The mass of the particleboard samples were measured using a digital weighing balance while the volume was calculated by multiplying the length (l) * breath (b) * height (h) of the samples.

#### 3.2.12.2 *Water absorption*

Water absorption test were performed on the particleboards according to ASTM D570 specification. The particleboard samples of dimensions 20 mm by 20 mm were weighed and then immersed in a distilled water bath at 25 $^oC$ for 24 hrs. The samples were taken out of the water and the surfaces dried with a clean dry cloth. The samples were then reweighed within 1min of removing them from water. The water absorption of each sample was calculated using Equation 3.6. The experiment was repeated twice for each sample and the results are shown in appendix B, Table B1.

Water absorption (%) $= \frac{(Wf - Wi)}{Wi} * 100$ (3.6)

Wi = Initial weight

Wf = Final weight

**3.2.12.3** ***Thickness swelling***

Thickness swelling test was performed on the particleboards according to ASTM D570 specification. The thickness of the particleboard samples were measured and then immersed in a distilled water bath at 25 $^{o}$C for 24 hrs. The samples were taken out of the water and the surfaces dried with a clean dry cloth. The thickness of the samples was then measured within 1min of removing them from water. The thickness swelling of each sample was calculated using Equation 3.7

Thickness swelling (%) $= \frac{(Tf - Ti)}{Ti} * 100$ (3.7)

Ti = Initial thickness

Tf = Final thickness

The experiment was repeated twice for each sample and the results are shown in appendix B, Table B2.

**3.2.12.4** ***Tensile test***

Tensile test was carried out using the Electronic Universal Testing machine Model WDW-100KN with model number 190536 according to ASTM D638 specification. The samples were cut into dumbbell shapes with dimensions 100 mm by 15 mm and the mid-section having 10 mm. Both ends were gripped on the machine and the machine was powered on, tension was applied to the samples at a constant speed of 20 $ms^{-1}$ until

it fractures. The tensile strength, elastic modulus and elongation were displayed on the computer screen connected to the machine and then recorded. Three tests were carried out for each sample and the average values were recorded. The stress-strain graphs and tensile properties can be seen in Appendix C.

#### 3.2.12.5 *Hardness test*

The Microvickers Hardness Tester model MV1-PC with machine number 07/2012-1329 was used for this experiment according to ASTM E384 standard test method. The samples were cut with dimensions 30 mm by 20 mm. The samples were placed directly under the indenter such that contact can be made between the sample and the indenter. The machine was powered on with a constant load of 0.3 kgf and maintained for a dwell time of 15 sec, the size of the resultant indentation was then measured with the help of a calibrated optical microscope and the hardness was evaluated as the mean stress applied underneath the indenter or the size of indentations. Three tests were carried out for each sample and the average hardness number was recorded. The results are shown in appendix B, Table B3.

#### 3.2.12.6 *Impact test*

The Charpy impact testing machine with model number 412-07-15269C and serial number HD9 6QD was used for this experiment according to ASTM A370. The samples were cut with dimensions 100 mm by 13 mm and notched 2 mm at the middle. The notched samples were then held in a cantilevered beam configuration, a swinging weight attached to a swinging pendulum held at a height was then released. The sample breaks at its notched cross-section upon impact, and the upward swing of the pendulum is used to determine the amount of energy absorbed in the process. Three tests were

carried out for each sample and the average energy absorbed was recorded. Results for impact test are shown in appendix B, Table B4.

### 3.2.13 Thermal analysis (TGA/DTA)

TGA/DTA was done using a PerkinElmer TGA 4000 thermogravimetric analyzer. The log was first filled out and the nitrogen gas was checked and put on, it was then connected to the instrument in the balance port. “Pyris” manager was opened and the TGA button at the top of the screen was selected. Using the tweezers supplied with the TGA, a clean empty crucible was loaded carefully with the wire basket (stirrup) onto the hang-down wire. The hangdown wire is connected to the microbalance at the top of the instrument. After the crucible has been installed, the “raise furnace” icon was selected. The furnace will move into position and rise up over the crucible. When the furnace is in position the “zero balance” icon was selected. When the balance is been satisfactorily zeroed, select the “cool furnace” icon to move the furnace out of the way. The sample stage was put in position under the crucible and hang down wire and carefully removed the crucible by lifting the wire basket from the hang down wire. The samples weighing 10 mg of bamboo at a constant heating rate of 10 $^{o}$C/min from room temperature usp to 850 $^{o}$C were put in the crucible and carefully reinstall the crucible and wire basket on the hang-down wire. The “raise furnace” icon was selected and allowed for the crucible with sample to stabilize for 10 min. While the sample stabilizes go to the method editor and edit as needed. In Method Editor, information about the sample was imputed. The weight of the sample was taken using the “weigh sample” icon. When the measurement was completed, the furnace was cooled and the crucible was removed.

### 3.2.14 Fourier transform infrared (FTIR)

The FTIR was done using the Agilent technology CARY 630 FTIR machine. The instrument was powered on and allowed to warm for 10-15 min, the computer attached to the instrument was also turned on. After initializing from the computer, the sampling operation was initiated and the method (absorbance or transmittance) selected. The crystal was cleaned with organic solvent and 10 mg of the sample placed in the crystal. Sample alignment check for blue line from red to green region for proper sampling was done and the sample identity was put for coding. The peaks were then selected for labeling on the system to acquire the wavenumbers as well as Transmittance and Absorbance (Lubis and Park, 2018)

# CHAPTER FOUR

## 4.0 RESULTS AND DISCUSSION

### 4.1 Thermal Analysis of Bamboo

The thermogravimetric analysis (TGA) shows the thermal degradation steps, the first TG curve labelled ‘a” in figure 4.1 corresponds to drying and dehydration between temperature ranges of 30 – 100 $^{o}$C. This stage is associated with slight mass loss.

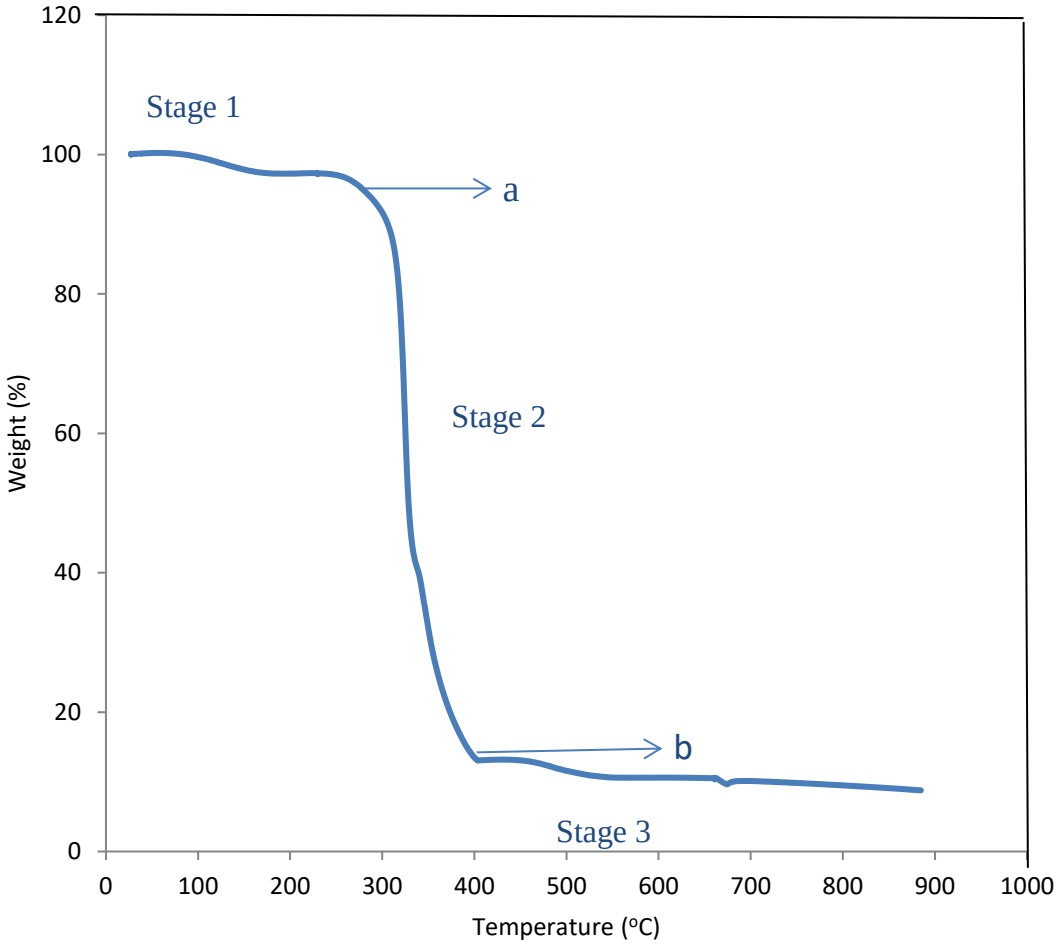


**Figure 4.1:** Thermogravimetric analysis (TGA) of Bamboo

The second curve labeled “b” covered temperature range of 250-390 $^{o}$C corresponding to weight losses as a result of hemicellulose and cellulose degradation (Mena *et al.*,

2014). At temperatures higher than 400 $^{o}$C which was the third and final stage, depolymerization of lignin occurs and this stage is associated with slow rate of degradation with less mass loss and high yield of char (Mahanim *et al.*, 2011). In general, pyrolysis of wood biomass occurs in a step-wise manner with hemicellulose breaking down first, cellulose next and then Lignin. From the DTA plot in Figure 4.2, the curve shows the pyrolysis of bamboo was an exothermic reaction because the area under the curve which is the enthalpy was negative. $T_{max}$ which corresponds to 317 °C represents the peak temperature where the rate of weight loss of bamboo was at a maximum or the maximum degradation rate for bamboo (Muigai *et al.*, 2020).

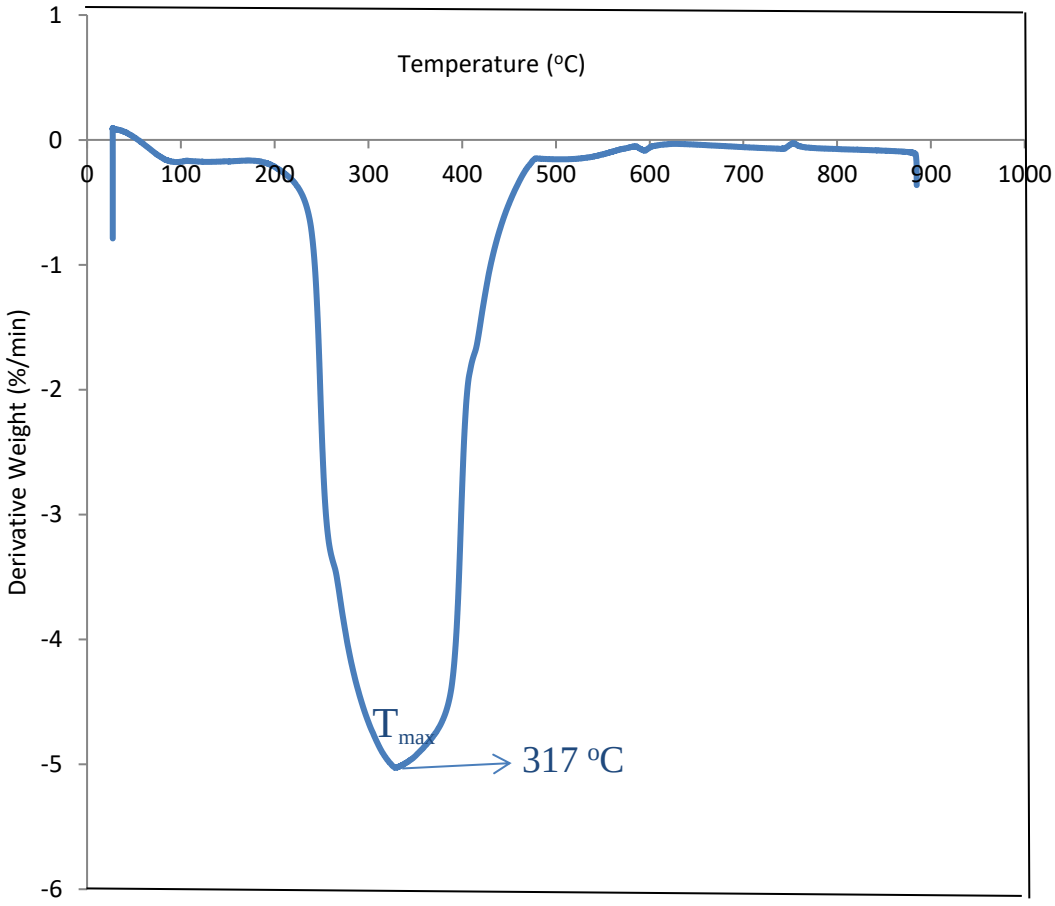


**Figure 4.2**: Differential thermal analysis (DTA) of Bamboo

### 4.2 Characterization of Bamboo

Analysis on the structural composition of the major components of bamboo was carried out on the bamboo samples as shown in Table 4.1. The results showed that the bamboo contains cellulose of 65.54 %. Percentage contents of lignin, hemicellulose and aqueous extracts were 18.79 %, 10.67 %, and 5 % respectively as shown in Table 4.1. These are in the range of hard wood biomass, Amaral and Leite (2014). A high percentage of cellulose in biomass suggests more volatilization during pyrolysis as both the polysaccharide structures were broken down at a lower temperature range of 200-400 °C (Sahoo *et al.,* 2021).

**Table 4.1: Composition of Bamboo**

| Component | Composition (%) |
|---|---|
| Cellulose | 65.54 |
| Hemicellulose | 10.67 |
| Lignin | 18.79 |
| Aqueous extracts | 5.00 |

### 4.3 Proximate and Ultimate Analysis of Bamboo

Proximate and Ultimate analysis were carried out on raw bamboo samples to determine moisture content, ash content, volatile matter and fixed carbon. The results are shown on Table 4.2. The high percentage of volatile matter, high fixed carbon, low moisture and ash from the proximate analysis meets the criteria of bamboo to be used as feedstock for biochar production and thus it is a potential precursor for pyrolysis. Lower

moisture contained in the bamboo results in less energy requirement during the pyrolysis process, less biomass consumption for the pyrolysis process and greater biochar yield. So biomass with a lower percentage of moisture is the most preferable feedstock for biochar production (Canal *et al*., 2020). The nitrogen and sulphur contents of the feedstock was 0.52 % and 0.08 % respectively which were significantly low, thus the content of NOx and SOx species which are environmental pollutants in the pyrolysis gas is expected to be very low.

**Table 4.2: Proximate Analysis of Bamboo**

| Moisture Content (%) | Ash Content (%) | Volatile Matter (%) | Fixed Carbon (%) |
|---|---|---|---|
| 10.24 | 1.85 | 74.15 | 14.73 |

**Table 4.3: Ultimate Analysis of Bamboo**

| Carbon (%) | Sulphur (%) | Nitrogen (%) | Hydrogen (%) | Oxygen (%) |
|---|---|---|---|---|
| 38.50 | 0.08 | 0.52 | 5.40 | 53.50 |

### 4.4 Proximate and Ultimate Analysis of Biochar

Tables 4.4 and 4.5 show the results for proximate and ultimate analysis of biochar produced at 400 $^{o}$C, 450 $^{o}$C and 500 $^{o}$C. The carbon content in all biochars increased with temperature. This is ascribed to the continuous evaporation of volatile matter. Higher pyrolysis temperature triggered thermal degradation reactions, dehydration, decarboxylation, and aromatization, which led to the enrichment of the carbon content

in the resulting biochar. These results were further confirmed by the significant decline of the volatile matter in biochar as the temperature rose from 400 °C to 500 °C. The higher amount of volatile matter at lower temperatures is ascribed to incomplete carbonization, which can be further correlated to the less amount of fixed carbon (Sahoo *et al*., 2021). Ash content increased with increase in temperature as a result of the mineralization of the mineral matter which was formed into ash during pyrolysis (Muigai *et al.,* 2020).

**Table 4.4: Proximate analysis of Biochar**

| Temp $^{o}$C | Moisture content (%) | Ash content (%) | Volatile Matter (%) | Fixed Carbon (%) |
|---|---|---|---|---|
| 400 | 1.90 | 3.05 | 19.40 | 45.65 |
| 450 | 1.54 | 3.26 | 19.30 | 45.60 |
| 500 | 1.38 | 3.56 | 19.10 | 46.96 |

**Table 4.5: Ultimate analysis of biochar**

| Temp. $^{o}$C | C (%) | H (%) | N (%) | O (%) |
|---|---|---|---|---|
| 400 | 54.82 | 6.18 | 0.24 | 15.06 |
| 450 | 55.62 | 5.03 | 0.25 | 10.45 |
| 500 | 56.48 | 3.88 | 0.22 | 6.37 |

### 4.5 Particle Size Analysis of Biochar

Analysis of the particle size of biochar are presented in Figure 4.3, the results show that the particle size distribution of biochar is wide and dispersive ranging from 5 to 1000

d.nm, the wide variation in the particle size is attributed to the structural composition of the raw feedstock (Muigai *et al.*, 2020). It can also be as a result of breaking down the biochar using the top-down approach of nanomaterial synthesis which was done in its solid state (Wu *et al*., 2017). Peak sizes of particles were recorded at 54.21 d.nm, 534.5 d.nm and 10.38 d.nm with 66.8 %, 20.5% and 11.5 %volume respectively. However, average particle size of nanobiochar was 115.3 d.nm.

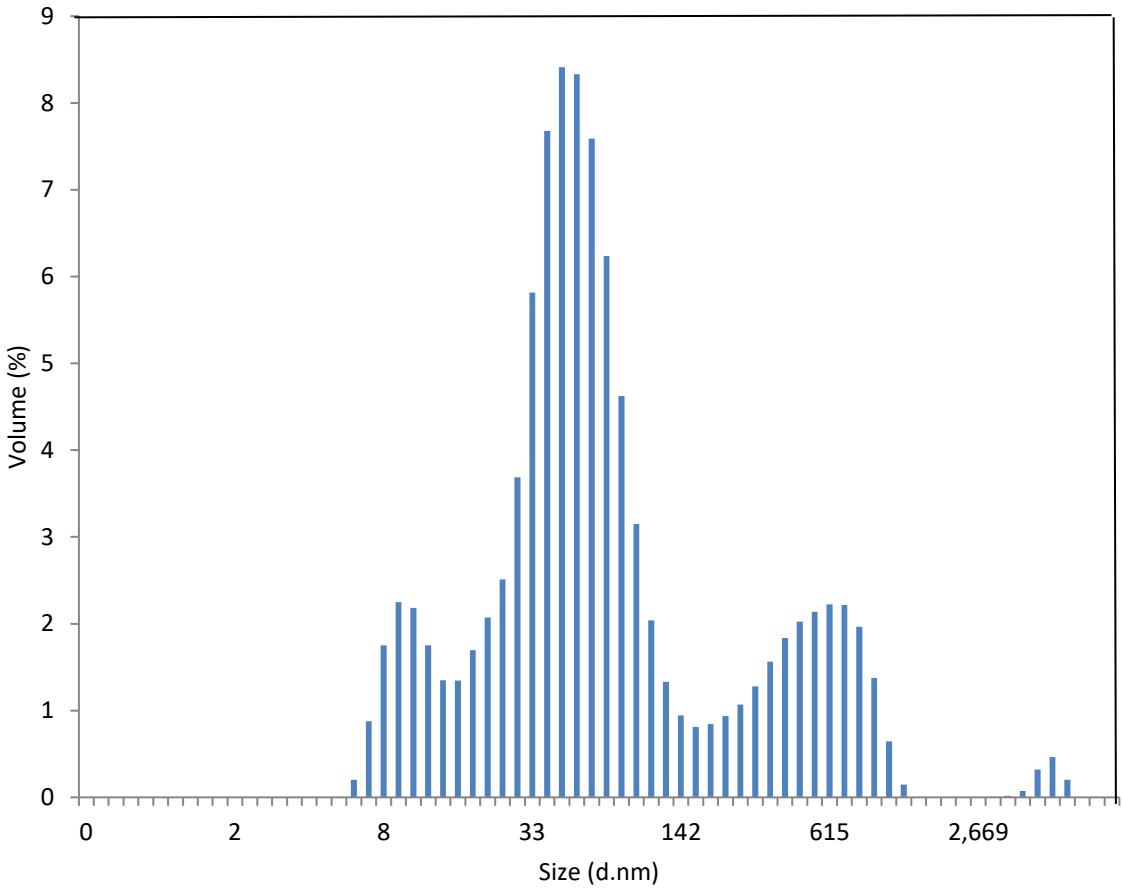


**Figure 4.3**: Particle size distribution of Nano biochar at 500 $^{o}$C

### 4.6 FTIR Spectroscopy for Bamboo and Nano Biochar

FTIR spectra of biochar and raw bamboo are shown in Figure 4.4. The peaks in the spectra corresponding to different functional groups are shown in Table 4.6. A

comparative evaluation of the FTIR spectra of the biochar at 500 ºC with raw biomass clearly showed the structural advancement of certain functional groups originally present in the feedstock after pyrolysis. The intensities of the peaks in range 3090 to 3311 $cm^{-1}$ (OH) appeared to be weak in the nano biochar when compared with that of the raw bamboo. This showed that an increase in temperature led to greater dehydration and decarboxylation (Guizani *et al*., 2017). The transmittance of the band at 2886 $cm^{-1}$ (ascribed to C- H) in raw bamboo and flattened in the nano biochar, which indicates the degradation of alcohol and carboxylic acid as a result of pyrolysis of bamboo (Chen *el al.*, 2015). The peak intensities in the range 1578 to 1593 $cm^{-1}$ corresponding to C=C and C=O indicates the presence of ketones which is a carbon containing substituent, the peak was stronger in the nano biochar as a result of higher carbon content after pyrolysis (Sahoo *et al*., 2021).

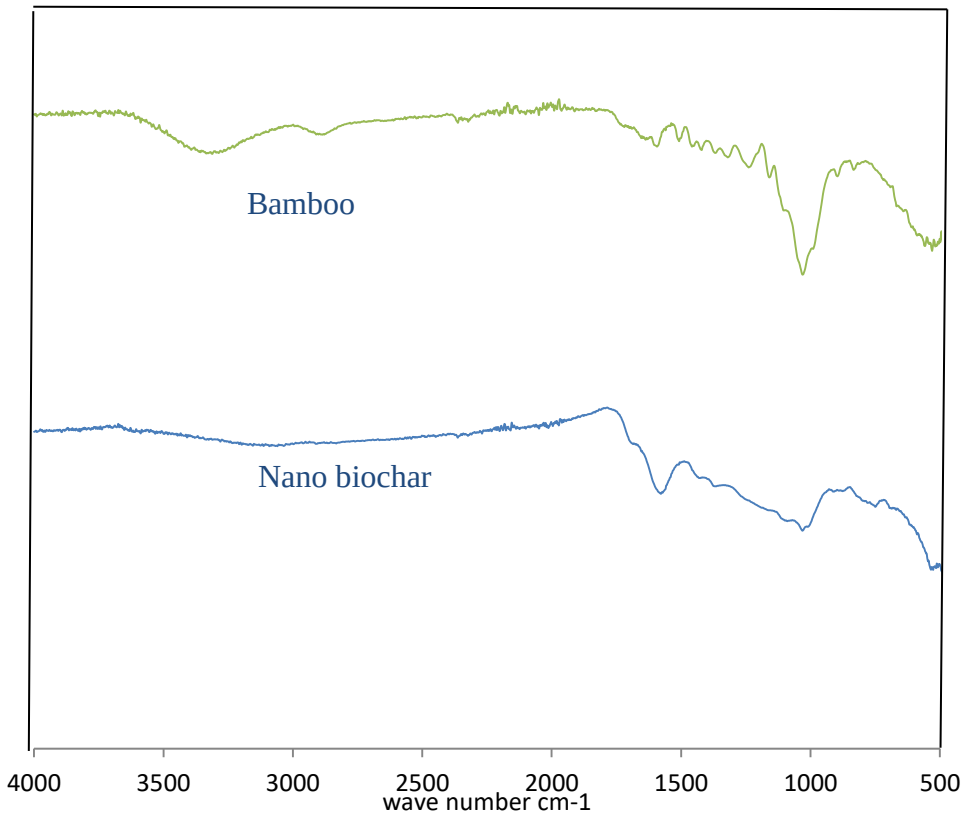


**Figure 4.4**: FTIR Spectra for bamboo and nano biochar at 500 ºC

The peak intensities in the range 1030 to 1031 $cm^{-1}$ that corresponded to C-O, C-C and C-C-O decreased after pyrolysis due to dehydration and degradation of the structural composition (decomposition of holocellulose) of the raw bamboo (Muigai *et al.*, 2020). The FTIR analysis showed the loss of carboxyl, hydroxyl, and carbonyl groups in raw bamboo during pyrolysis leaving behind carbon rich biochars.

**Table 4.6: Classification of functional groups of Bamboo and nano biochar from FTIR Spectra**

| Wavenumber ($cm^{-1}$) | | Functional group | Class of compound |
|---|---|---|---|
| Bamboo | Nano biochar | | |
| 3311 | - | O-H | Hydroxyl |
| - | 3090 | O-H | Hydroxyl |
| 2886 | - | C-H | Aliphatic |
| 1593 | - | C=C, C=O | Ketones |
| 1570 | 1578 | C=C, C=O | Ketones |
| 1030 | 1031 | C-O | Cellulose, Hemicellulose and Lignin |

### 4.7 Physicochemical Properties of Urea Formaldehyde Resin

Some physical and chemical properties of neat and modified UF resins are shown in Table 4.7. UF-0, UF-1, UF-2 and UF-3 corresponding to neat resin, resins modified with nano biochars at 400 ºC, 450 ºC and 500 ºC respectively. The unmodified UF resin was cream in colour while the modified UF resin samples had dark colours due to the introduction of biochar which contains carbon black. There was no significant increase in the pH values of the modified resin samples as compared to the neat UF sample. There was a slight increase in percentage solid content of neat UF resin as compared to the modified UF resin, this could be as a result of the introduction of biochar which is a solid product of pyrolysis into the UF resin.

**Table 4.7: Physicochemical Properties of Neat and Modified UF Resin**

| Parameter | UF-0 | UF-1 | UF-2 | UF-3 |
|---|---|---|---|---|
| Viscosity (cps) | 150 | 152 | 151 | 154 |
| Solid content (%) | 60 | 65 | 63 | 64 |
| Gel time (s) | 58 | 59 | 58 | 60 |
| Density ($g/cm^3$) | 1.28 | 1.35 | 1.30 | 1.30 |
| pH | 7.8 | 8.0 | 7.9 | 8.0 |
| Appearance | Cream | Black | Black | Black |

The Gel time of the modified UF resin samples did not change significantly when compared with the neat UF resin. There was a slight increase in the viscosity and density of modified UF resin samples as against the neat UF resin sample. Studies have shown that, as the viscosity of UF adhesive increases, so does the adhesion bonding

strength. This situation is explained by the increase of molecular weight and crosslink density of the modified UF resin (Bardak *et al.*, 2018).

### 4.8 Thermal Analysis of Urea Formaldehyde Resin

The TGA/DTA curves of unmodified and nano biochar modified UF resins are shown in Figures 4.5 and 4.6. The TGA curves of the neat and modified UF resin are simultaneously displayed in Figure 4.5, both curves indicates that the pyrolysis process of the resin is in three stages. The first stage from the TGA curve denotes dehydration and partial volatilization, the water is present as a result of water addition during synthesis of the resin or as a result of condensation reactions during synthesis.

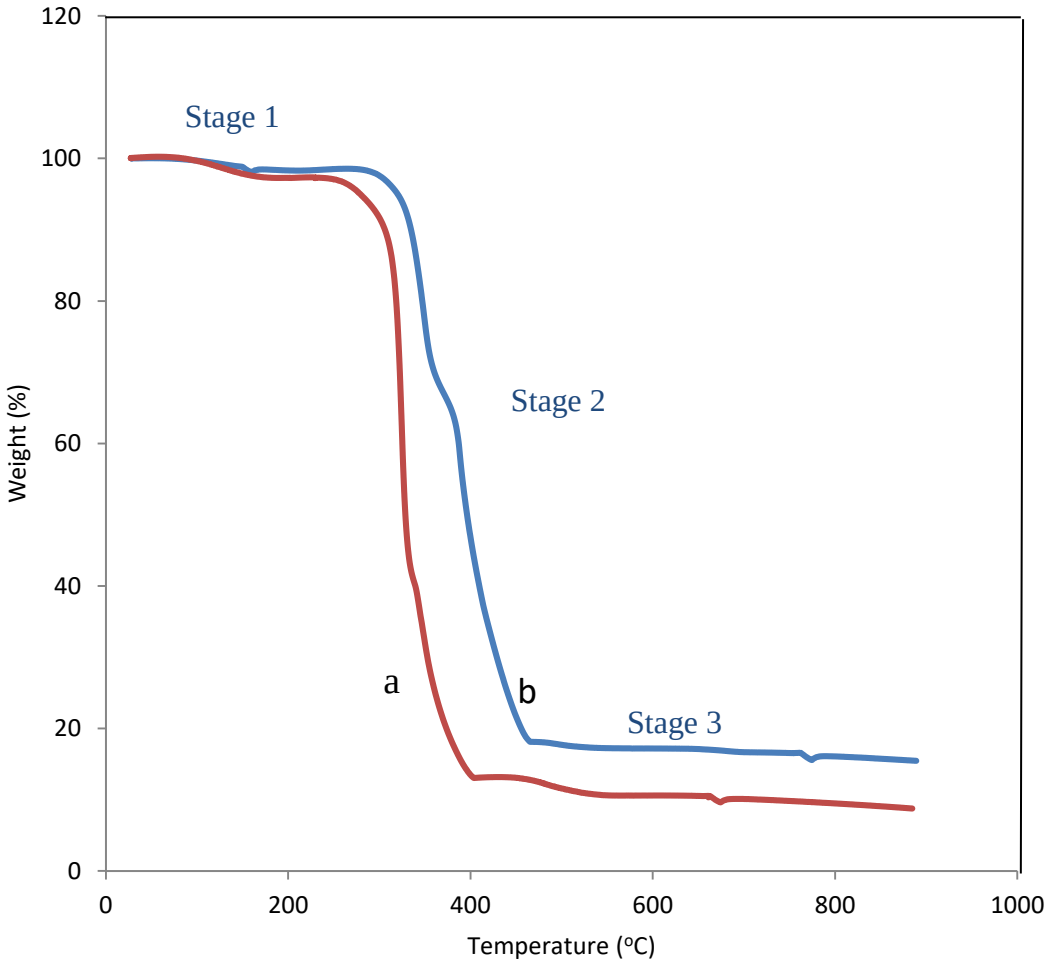


**Figure 4.5**: TGA of (a) neat and (b) modified UF resin

The second stage indicates flash pyrolysis partly due to release of formaldehyde accompanied with water. The third stage is associated with slow decomposition of the resin (Li *et al*., 2014). It can also be seen from the DTA curves in Figure 4.6 that weight loss ratio of modified UF resin sample was lower than that of unmodified resin. This can be seen from the peak temperatures of degradation Tmax indicated for both neat and modified UF resin which was 336 °C and 375 °C respectively. This showed that heat stability of UF resin increased significantly after modification thereby making it more thermally stable (Hong *et al*., 2016).

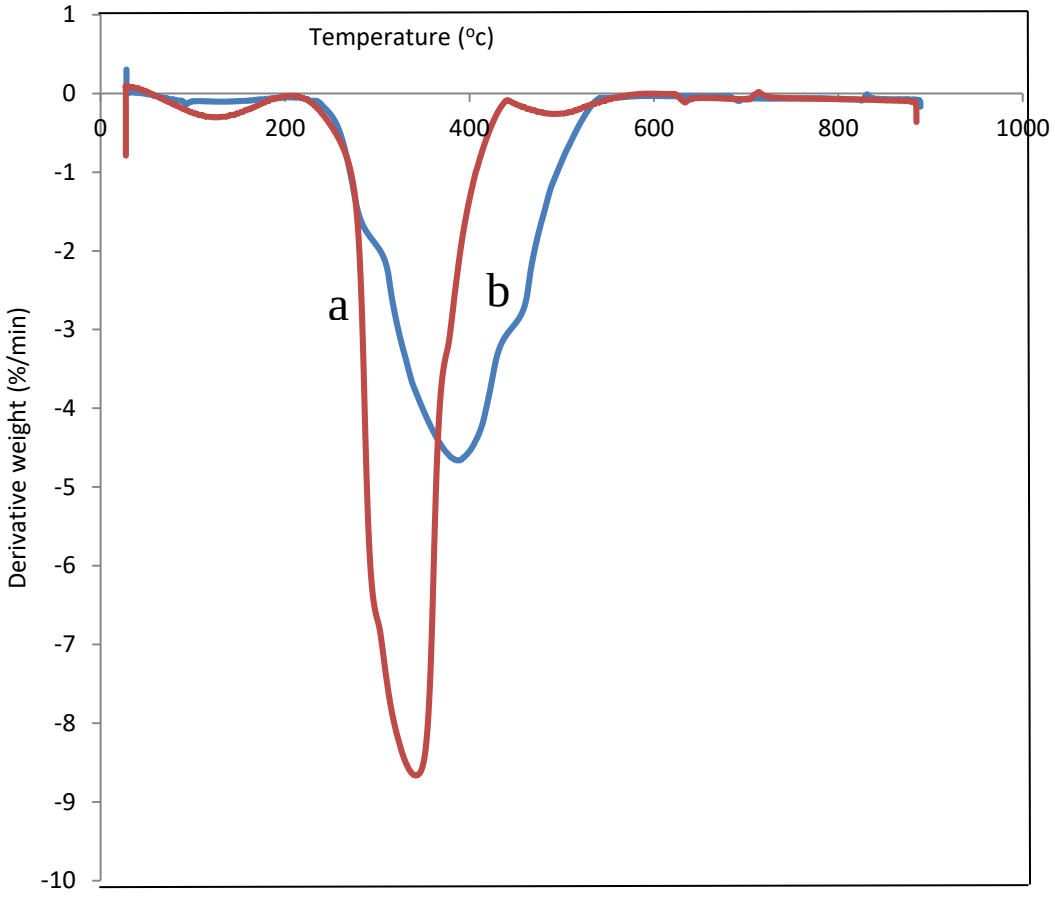


**Figure 4.6**: DTA of (a) neat and (b) modified UF resin

### 4.9 FTIR Spectroscopy of Urea Formaldehyde Resin

Figure 4.7 shows the FTIR spectra for neat and nano biochar modified UF resins. Their corresponding classifications of functional groups are shown in Table 4.8. The spectra of the neat and modified UF resins were almost identical as shown in Figure 4.7, the absorption peak at 3332 $cm^{-1}$ was assigned to the O-H stretching modes. The modified resins showed sharper characteristic absorption peaks in this region. The sharpness of these bands indicated a reduction in the extent of hydrogen bonding interaction, which was expected because the structure was more cross-linked (Li *et al*., 2014). The bands at 1625 $cm^{-1}$ was assigned to the C=O stretch. The bands observed at 1461 $cm^{-1}$ was due to C – H bend, the absorption peaks at 1349 $cm^{-1}$ and 1259 $cm^{-1}$ corresponded to C = O groups. The observed bands at 1114 $cm^{-1}$ was due to the C – O – C groups.

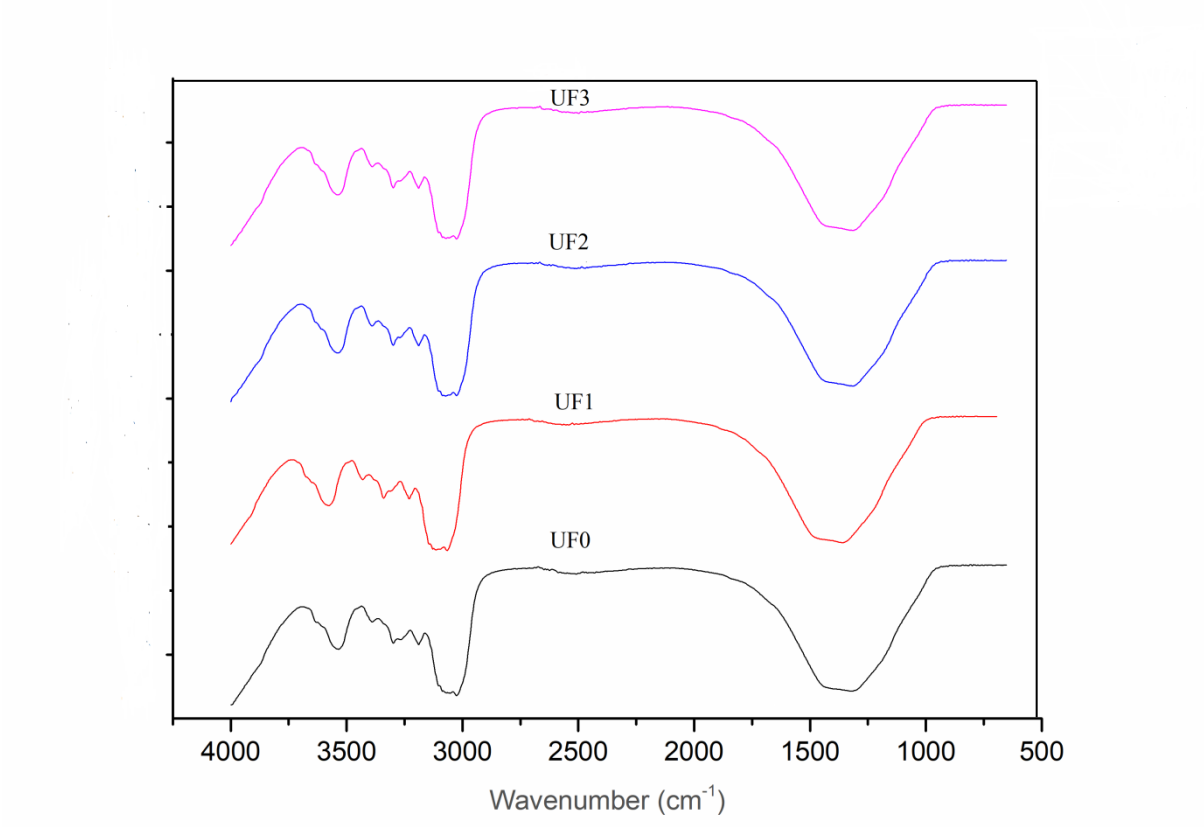


**Figure 4.7**: FTIR Spectra for neat (UF0) and modified UF resins (UF1, UF2 and UF3)

**Table 4.8: Classification of functional groups of neat and modified UF resin**

| Wavenumber ($cm^{-1}$) | Functional group | Class of compound |
|---|---|---|
| 3332 | O-H | Carboxylic acids |
| 1625 | C=O | Amides |
| 1461 | C-H | Alkanes and Alkynes |
| 1114 | C-O-C | Ethers |

## 4.10 Physical and Mechanical Properties of Particle Boards

### 4.10.1 Density

Calculated values for density of neat and modified particle boards are shown on Table 4.9. Samples S0, S1, S2 and S3 corresponds to particle boards produced with neat resin and nano biochar modified resins at 400 $^{o}$C, 450 $^{o}$C and 500 $^{o}$C respectively. The densities of neat particleboard sample S0 and modified particleboard samples S1, S2 and S3 are in the range of 0.68 to 0.72 g/$cm^3$. These boards can be classified as low density particleboards because they fall within the JIS standard of 0.4 to 0.9 g/$cm^3$ for low density particleboards (Astari *et al.*, 2018).

**Table 4.9: Densities of neat and modified particleboards**

| Sample | S0 | S1 | S2 | S3 |
|---|---|---|---|---|
| Density (g/$cm^3$) | 0.68 | 0.76 | 0.72 | 0.68 |

### 4.10.2 Water absorption

The results for water absorption as presented in appendix B, Table B1 and plotted in Figure 4.8 showed that there was a reduction in water absorption of modified samples S1, S2 and S3 corresponding to 35.04 %, 32.13 % and 33.93 % respectively when compared to the neat sample S0 which had water absorption of 37.06 %. This may be as a result of the hydrophobic nature of the modified UF resin brought about by the strong intermolecular cohesive bonding within the molecules of the modified UF resin which prevented water from penetrating the samples made from the modified resin (Ejiogu *et al.*, 2018).

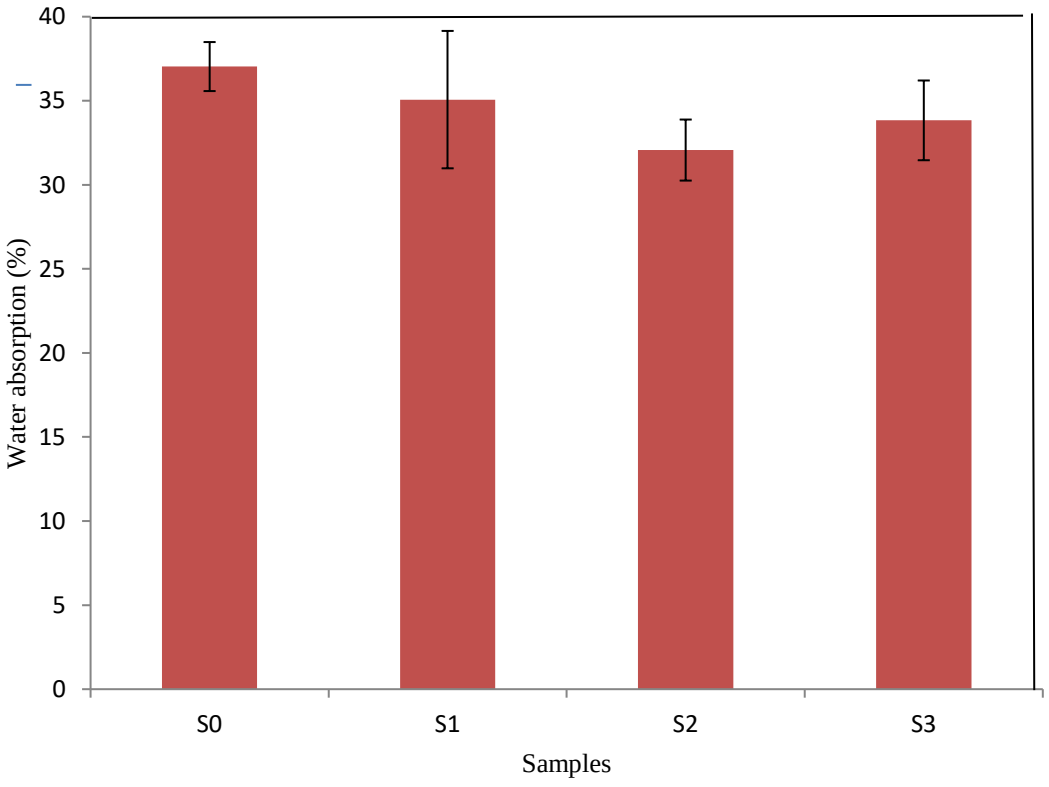


**Figure 4.8**: Water absorption of neat and modified particleboards

### 4.10.3 Thickness swell

Thickness swelling was determined to show the stability of dimension for particleboards, as presented in appendix B, Table B2 and plotted in Figure 4.9. All modified samples S1, S2 and S3 showed a significant decrease in thickness swell of 43.33 %, 40 % and 43.52 % respectively when compared to the neat particleboard sample S0 which has a thickness swell of 46.67 %. Thickness swelling showed a direct relationship to the results obtained on water absorption. This may be due to the presence of nano biochar in the modified samples which possesses hydrophobic properties on the particleboard as reported by (Astari *et al*., 2018).

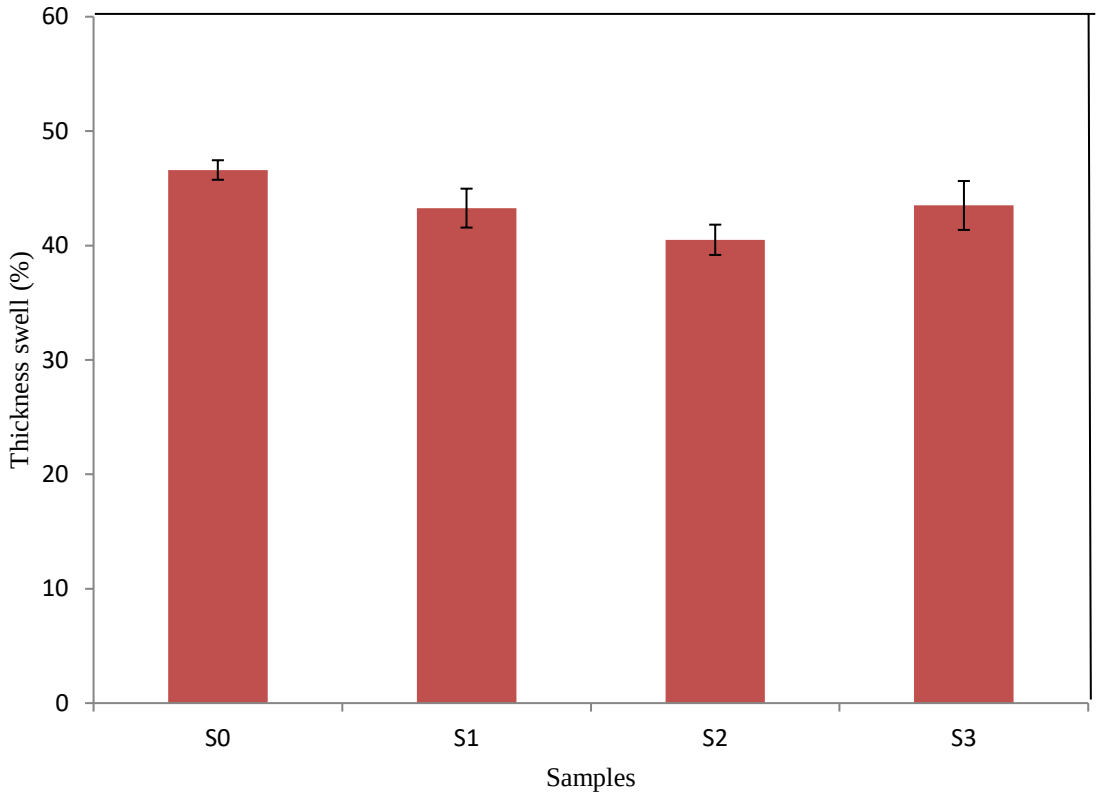


**Figure 4.9**: Thickness swell of neat and modified particleboards

The lower the percentage of thickness swelling, the better the particleboard performance. Particle board samples with low density tend to have high porosity. This

low density is why water quickly enters the pores of particleboard so that water will break the bond between filler, fiber, and matrix (Lusiani *et al.*, 2020).

### 4.10.4 Tensile strength

The results for tensile strength as shown on Figure 4.10 showed an increase in tensile strength for modified samples S1 and S2 having tensile strength of 21.29 MPa and 25.16 MPa compared with the neat sample S0 with tensile strength of 15.54 MPa. The performance of tensile strength of the particleboard is generally affected by parameters like tensile properties of its components (particle and matrix),

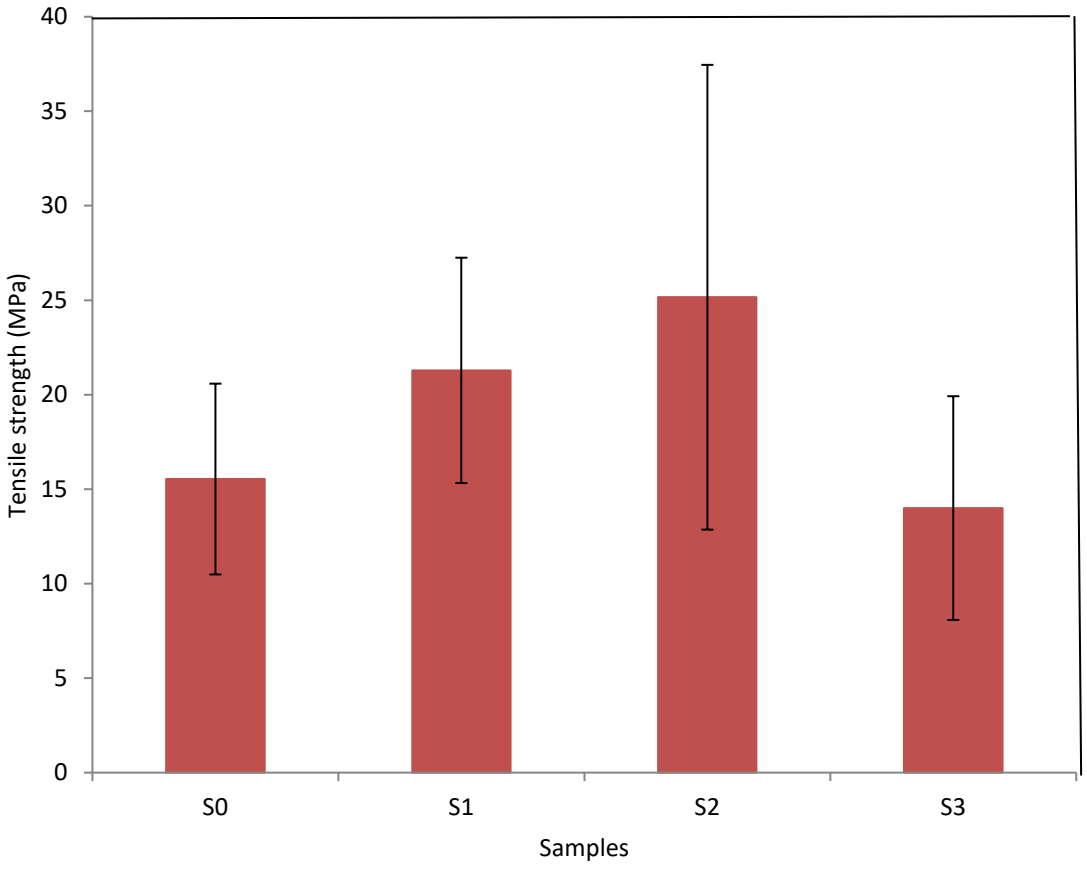


**Figure 4.10**: Tensile strength of neat and modified particle boards

it can be concluded that the nano biochar particles have improved mechanical performance especially tensile properties of the particleboard due to its extremely large

surface area and its smooth nonporous surface, which indicated that the addition of nano biochar particles was able to increase stiffness as the particles fill in the voids in the particleboard and minimized the agglomeration (Fong *et al*., 2018). The stress-strain graphs and other tensile properties for the samples are presented in appendix C.

### 4.10.5 Elastic modulus

Elastic Modulus of neat and modified particleboards samples represented in Figure 4.11 shows an increase in the elastic modulus of modified samples S1, S2 and S3 corresponding to 12.53 MPa, 19.83 MPa and 11.01 MPa respectively when compared to the neat particleboard sample having elastic modulus of 10.42 MPa. Elastic modulus is affected by several factors such as adhesive content, adhesive type, bonding performance and fiber length (Astari *et al*., 2018). High stiffness properties normally resulted in higher elastic modulus values. Boards with low elastic modulus tend to be ductile or flexible and brittle when the elastic modulus value is high (Wahab *et al*., 2018).

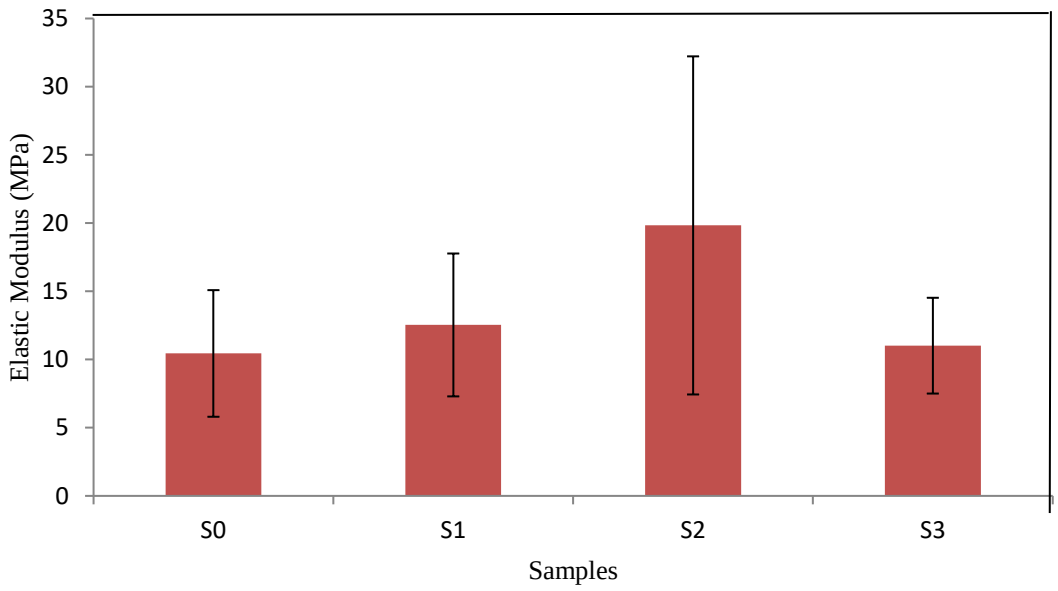


**Figure 4.11**: Elastic Modulus of neat and modified particleboards

### 4.10.6 Elongation

Results for elongation of particleboard samples represented in Figure 4.12 showed that there was no significant difference in elongation of modified sample S1, S2 and S3 corresponding to 84.6 %, 84 % and 85.4 % when compared to neat particleboard sample with elongation 84.4 %. The low elongation shown by samples S2 and S3 indicates that the samples may become brittle so that particleboard characteristics are natural to break when the load exceeds its strength.

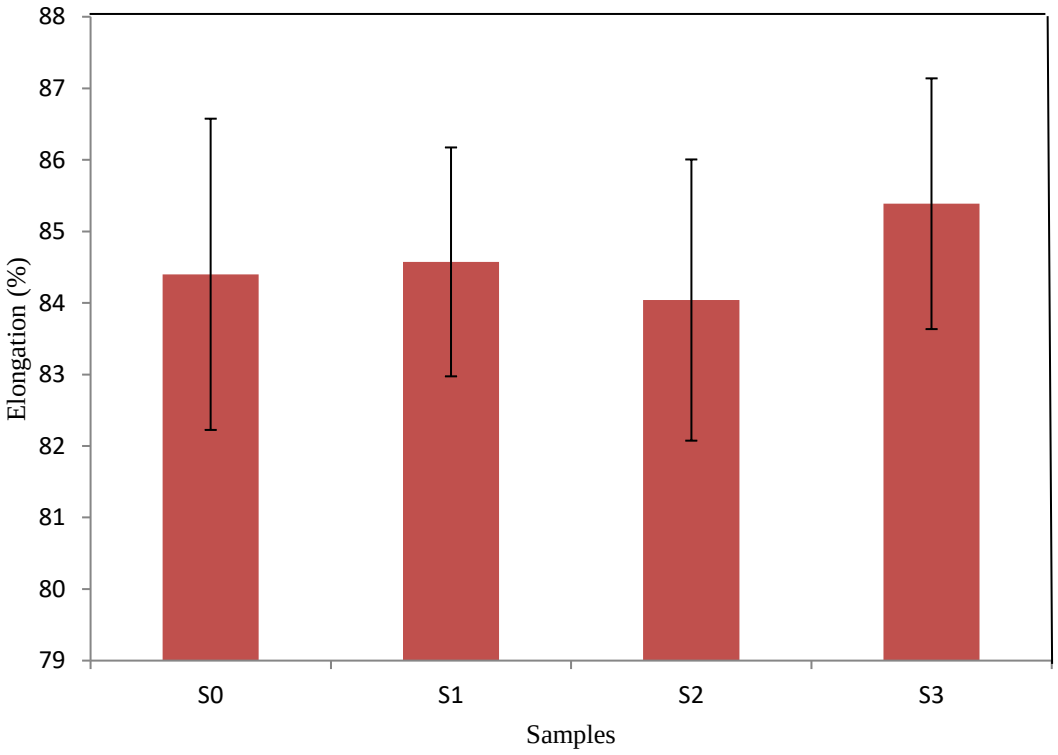


**Figure 4.12**: Elongation of neat and modified particleboards

### 4.10.7 Hardness test

The hardness number of neat and modified particleboard samples as represented in appendix B, Table B3 and plotted in Figure 4.13 shows an increase in the hardness of modified samples S1, S2 and S3 corresponding to 25.3 HV, 29.1 HV and 44.9 HV respectively when compared to the neat particleboard sample S0 having a hardness number of 25.0 HV.

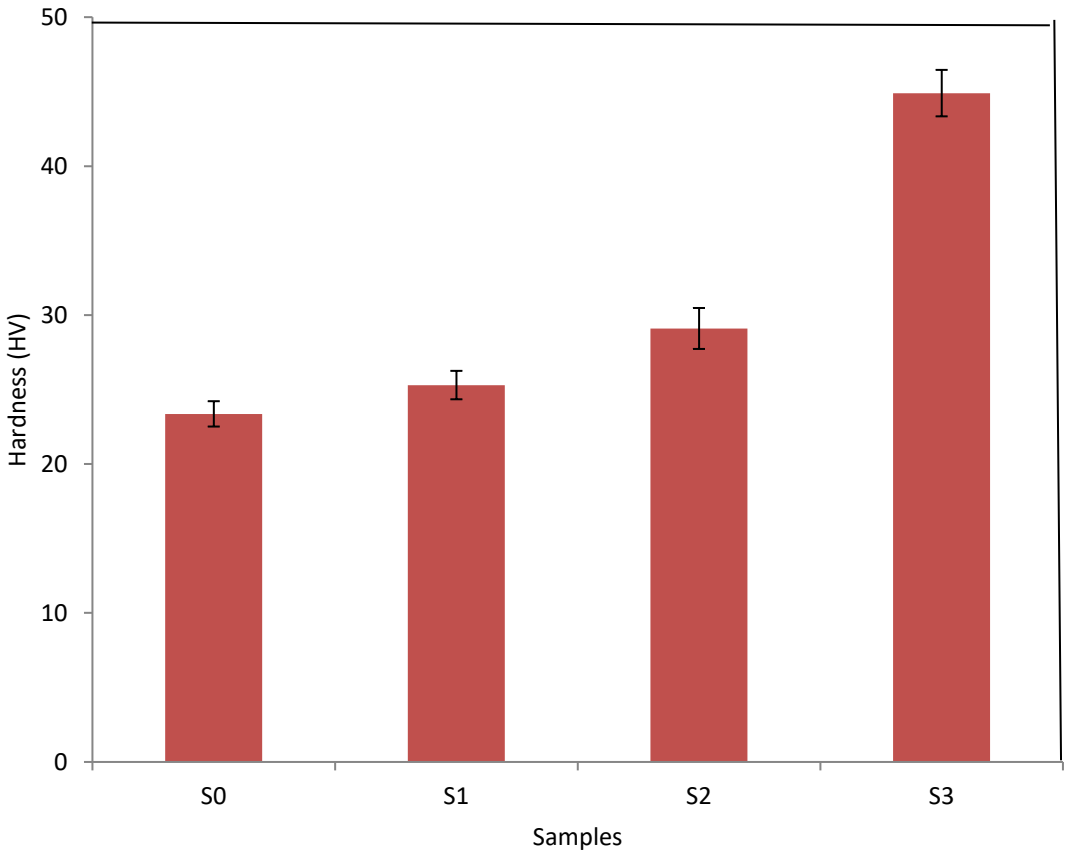


**Figure 4.13**: Hardness of neat and modified particleboards

This hardness depends directly on the pores formed on the particle board during the manufacturing process. The filler distribution pattern in the composite will affect the mechanical properties of the particleboard. The homogeneous distribution of fillers can

provide higher hardness and strength than the distribution of fillers that are not uniformly formed. This filler distribution can be studied from hardness at any point in the material surface. If the hardness at any point has the same value, it is said that filler distribution is uniform (Lusiani *et al*., 2020).

### 4.10.8 Impact test

Impact values of neat and modified particleboards are represented in appendix B, Table B4 and plotted in Figure 4.14. There was an increase in the impact energy for modified samples S2 and S3 corresponding to 0.27 J and 0.32 J when compared with neat particleboard sample S0 and modified sample S1 corresponding to 0.25 J and 0.22 J respectively.

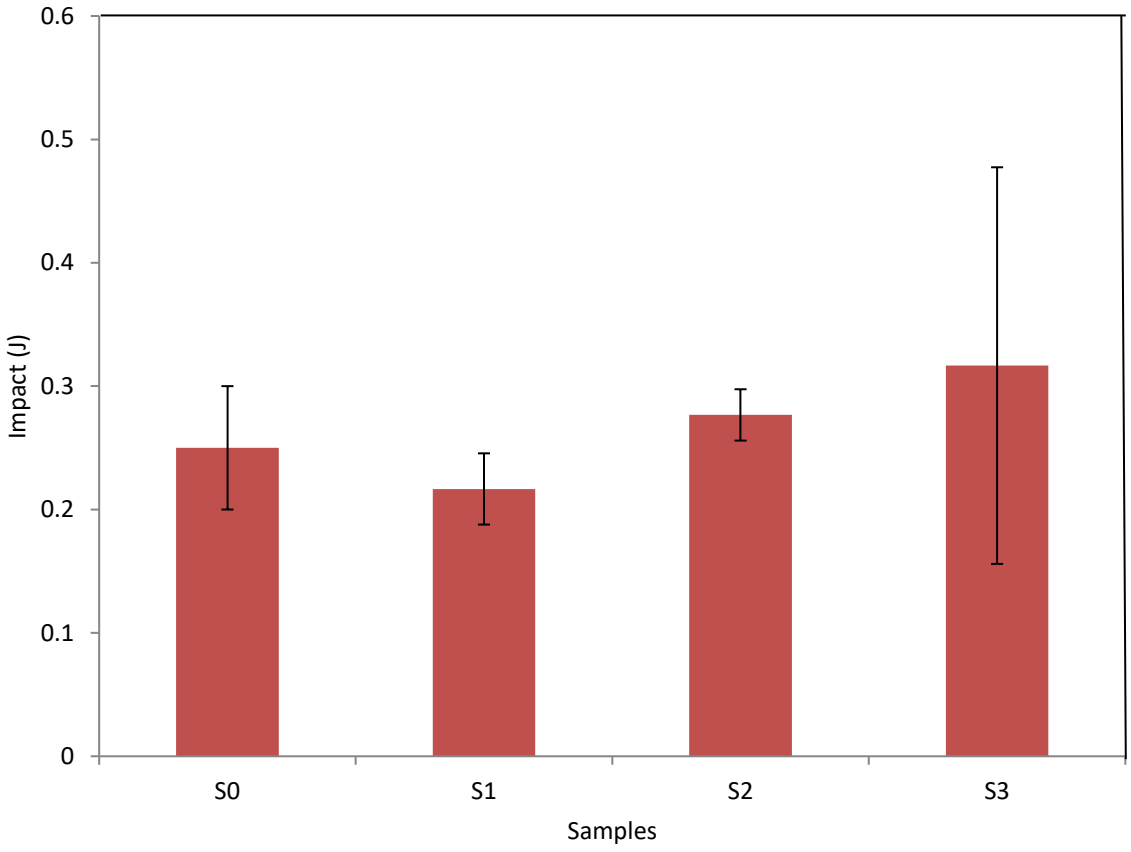


**Figure 4.14**: Impact of neat and modified particleboards

Impact strength of the particleboard is greatly influenced by the particle size, fibre distribution, particle orientation and particle-polymer adhesion. The nano biochar modified particleboard was able to withstand fast impact load better than the unmodified sample because the particles tend to slip from matrix and left weak points or stress on concentrated area corresponding to what was reported by (Chiang *et al*., 2016).

# CHAPTER FIVE

## 5.0 CONCLUSION AND RECOMMENDATIONS

### 5.1 Conclusion

Bamboo constitutes a very good feedstock for biochar production by pyrolysis process as shown by volatile matter content of 74.15 %. Physical properties of bamboo and nano biochar which includes moisture content, volatile matter, ash content and fixed carbon were evaluated and results showed that nano biochar pyrolyzed at 500 $^{o}$C contains the highest fixed carbon content of 46.96 % and least moisture content of 1.38 %. Chemical properties which include carbon, oxygen, hydrogen, sulphur and nitrogen contents were also evaluated, results showed that percentage carbon increases as pyrolysis temperature is increased. The physical and chemical properties changed significantly with increase in pyrolysis temperature. The produced nano biochar featured low ash content and stable carbon content making the biochar a suitable matrix for the synthesis or production of composites.

Urea formaldehyde resin was successfully synthesized using the alkaline-acid method and modified with nano biochar produced from pyrolysis of bamboo. Physical and chemical properties of the neat and modified UF resins were investigated and compared. The incorporation of nano biochar into the UF resin significantly altered the resin basic properties such as viscosity, solid content, gel time, density, pH and appearance. The viscosities of the modified resins increased to 152 cps, 151 cps and 154 cps respectively as against the neat resin which had a viscosity of 150 cps. The solid content also increased significantly ranging from 63-65 % for modified resins while the neat resin had a solid content of 60 %. Gel time, density and pH of both neat and modified resins

did not change significantly with gel time ranging between 58 to 60 sec, densities of between 1.28 to 1.35 g/cm3 and pH ranging from 7.8 to 8.0.

The neat and modified UF resins were used to produce particleboards using saw dust as filler. Physical and mechanical properties of the particleboards which include density, water absorption, thickness swell, tensile test, hardness test and impact test were evaluated. The densities of the particleboards produced falls within the range of 0.68 $g/cm^3$ to 0.76 $g/cm^3$ which falls within the range of low density particleboard. Particleboard produced with sample UF2 showed the highest water resistance and least thickness swell of 32.13 % and 40 % respectively. It also showed the highest values in tensile strength of 25.16 MPa and elastic modulus of 19.83 MPa which may be due to its extremely large surface area and its smooth nonporous surface. Particleboards produced with sample UF3 gave the highest hardness of 44.9 HV and impact energy of 0.32 J. These particleboards can be used as a substitute for plywood panels because they fall within the JIS standard for low density particleboard.

## 5.2 Recommendations

i. Other methods of biochar synthesis should be studied and explored in order to address the issue of cost associated with pyrolysis.
ii. Optimization should be carried out in the application of nano biochar modified Urea Formaldehyde resin in other to ascertain the required formulation for achieving desired properties.

## 5.3 Contribution to Knowledge

i. Biochar was produced using bamboo as feedstock by pyrolysis process using a locally fabricated pyrolysis reactor at temperatures of 400 $^{o}$C, 450 $^{o}$C and 500 $^{o}$C. Biochar pyrolyzed at 500 $^{o}$C contained the highest fixed carbon content of 46.96 % and least moisture content of 1.38 %.

ii. Urea formaldehyde resin was successfully synthesized using the alkaline-acid method and modified with nano biochar produced from pyrolysis of bamboo. The incorporation of nano biochar into the UF resin significantly altered the resin basic properties, the viscosities of the modified resins increased to 152 cps, 151 cps and 154 cps respectively as against the neat resin which had a viscosity of 150 cps.

iii. The neat and modified UF resins were used to produce particleboards using saw dust as filler. The densities of the particleboards produced falls within the range of 0.68 g/cm$^3$ to 0.76 g/cm$^3$ which falls within the range of low density particleboard.

## REFERENCES


Abdellaoui, H., Raji, M., Essabir, H., Bouhfid, R., & Qaiss, A. (2019). Mechanical behavior of carbon/natural fibre-based hybrid composites. *Moroccan Foundation for Advanced Science, Innovation and Research.*

Agrawal, A. & Yi, G. (2020) Sample pretreatment with graphene materials. *Comprehensive Analytical Chemistry,* 91, 21-47.

Ahmed, A., Bakara, M.S., Hamdania, R., Park, Y., Lam, S., Sukrie, R.S., Hussain, M., Majeed, K., Phusunti, N., Jamil, F., & Aslam, M. (2020). Valorization of underutilized waste biomass from invasive species to produce biochar for energy and other value-added applications. *Environmental Research* 186, 109596.

Alam, D., Rahman, K., Ratul, S.B., Sharmin, A., Islam, T., Hasan, A.W.. & Islam, N. (2015). Properties of Particleboard Manufactured from Commonly Used Bamboo (*Bambusa vulgaris*) Wastes in Bangladesh. *Advances in Research,* 4(3), 203-211.

Amaral, S., & Leite, L. (2014). Comparative Study for Hardwood and Softwood forest Biomass; Chemical Characterization, combustion phases and gas and Particulate Matter Emissions. *Bioresource Technology*, 164, 55-63.

Astari, L., Prasetiyo, L.K.W., & Suryanegara, L. (2018). Properties of Particleboard Made from Wood Waste with Various Sizes. *In IOP Conference Series: Earth and Environmental Science* 166, 1(012004).

Bardak, T., Sozen, E., Kayahan, K., & Bardak, S. (2018). The impact of Nanoparticles and moisture content on bonding strength of Urea formaldehyde Resin Adhesive. *DRVNA INDUSTRIJA*, 69(3) 247-252.

Bartoli, M., Nasir, M.A., Jagdale, P., Passaglia, E., Spiniello, R., Rosso, C., Giorcelli, M., Rovere, M., Tagliaferro, A. (2019). Influence of pyrolytic thermal history on olive pruning biochar and related epoxy composites mechanical properties. *Journal of Composite Materials,* 54(14), 1863–1873.

Bharath, K.N., & Swamy, R.P. (2009). Adhesive Tensile And Moisture Absorption Characteristics of Natural Fibres Reinforced Urea Formaldehyde Composites. *International Journal of Recent Trends in Engineering.* 1,(5).

Biswas, S., Shahinur, S., Hasan, M. & Ahsan, Q. (2015). Physical, Mechanical and thermal properties of Jute and Bamboo Fibre Reinforced Unidirectional Epoxy composites. *Sixth BSME International Conference on Thermal Engineering (ICTE 2014). Procedia Engineering* (105), 933-939.

Bodur, M., Bakkal, M. & Sonmez, H. (2016). The effects of different chemical treatment methods on the mechanical and thermal properties of textile fibre reinforced polymer composites. *Journal of Composite Materials,* 0(0),1-14.

Boran, S., Usta, M., & Gumuskaya, E. (2011). Decreasing formaldehyde emission from medium density fiberboard panels produced by adding different amine compounds to Urea formaldehyde resin. *International Journal of Adhesion and Adhesives* (31), 674-678.

Canal, W.D., Carvalho, A.M.M., Figueiro, C.G., Carneiro, A.D.C.O., Fialho, L.D.F., Donato, D.B. (2020). Impact of wood moisture in charcoal production and quality. *Florest. Ambient.* 27, http://doi.org/10.1590/2179-8087.099917.

Candan, Z., & Akbulut, T. (2013). Developing environmentally friendly wood composite panels by Nanotechnology. "Nano wood composites", *BioResources* 8(3), 3590-3598.

Chen, D., Liu, D., Zhang, H., Chen, Y., & Li, Q. (2015). Bamboo Pyrolysis using TG-FTIR and a lab scale reactor: Analysis of pyrolysis behaviour, product properties and energy yield. *Fuel* (148), 79-86.

Chiang, T.C., Hamdan, S., & Osman, M.S. (2016). Mechanical Strength of Sago/Urea Formaldehyde Particleboard Affected by the Particle Size. *Applied Mechanics and Materials.*833, 3-10.

Dinte, E., & Sylvester, B. (2018). Adhesives: Applications and Recent Advances. *Applied Adhesive Bonding in Science and Technology. Adhesives:* http://dx.doi.org/10.5772/intechopen.71854.

Dotun, A.O., Adesoji, A.A., Oluwatimilehin, A.C. (2018). Physical and Mechanical Properties Evaluation of Particle Board Produced From Saw Dust and Plastic Waste. *International Journal of Engineering Research in Africa* (40), 1-8.

Ejiogu, I.K., Odiji, M.O., Ayejagbara, M.O., Shekari, T.N.B. & Ibeneme, U. (2018). Mechanical properties of urea formaldehyde particleboard composite. *American Journal of Chemical and Biochemical Engineering*, 2(1), 10-15.

Ezeribe, A.I., Bello, K.A., Adamu, H.M., Boryo, D.E.A. & Pan, O. (2014). Effects of temperature and catalyst mass on the mechanical properties of Urea formaldehyde Resinated cotton fabrics. *IOSR Journal of Engineering (IOSRJEN)* (4), 49-55.

Fong, A.L., Khandoker, N.A.N. & Debnath, S. (2018). Development and characterization of sugarcane bagasse fiber and nano-silica reinforced epoxy hybrid composites. *IOP Conf. Series: Materials Science and Engineering* 344 012029 doi:10.1088/1757-899X/344/1/012029.

Ghyselsa, S., Ronssea, F., Dickinson, D., & Prins, W. (2019). Production and characterization of slow pyrolysis biochar from lignin-rich digested stillage from lignocellulosic ethanol production. *Biomass and Bioenergy*, 122, 349–360.

Guizani, C., Jeguirim, M., Valin, S., Limousy, L., & Salvador, S. (2017). Biomass chars: The Effects of Pyrolysis Conditions on Their Morphology, Structure, Chemical Properties and Reactivity. *Energies*, 10(6), 796.

Gupta, G., Kumar, A., Tyagi, R., & Kumar, S. (2016). Application and Future of Composite Materials: A Review. *International Journal of Innovative Research in Science, Engineering and Technology.* (5), 5.

Hisham, A.E., Tawfik, M.E., & Elsayed, N.H.,(2011). Effects of addition of Glycolysis products of poly(ethylene-terephthalate) wastes to Urea-formaldehyde resin on its adhesion performance to wood substrates and formaldehyde emission. *Journal of Applied Polymer Science*, (123), 2377-2383.

Hong, W., Meng, M., Gao, D., Liu, Q., Kang, C., Huang, S., Zhou, Z., & Chen, C. (2016). Thermal Analysis Study of Modified Urea-Formaldehyde Resin. *Polymer (Korea),*40(5), 707-713.

Huynh, K., Pham, X., Kim, J., Lee, S.H., Chang, H., Rho, W., & Jun, B. (2020). Synthesis, Properties, and Biological Applications of Metallic Alloy Nanoparticles. *International Journal of Molecular Sciences,* 21(14), 5174.

Iždinský, J., Vidholdová, Z., & Reinprecht, L. (2020). Particleboards from Recycled Wood. *Forests* 11(11), 1166.

Joakim, J. (2012). Investigation of Urea-formaldehyde Resins, the effects of the formaldehyde/urea mole ratios during synthesis. *Master of Science Thesis, Stockholm, Sweden.*

Kandelbauer, A., Despres, A., Pizzi, I., & Taudes (2007). Testing by fourier transform infrared species variation during Melamine-Urea-Formaldehyde Resin preparation. *Journal of Applied Polymer Science* (106) 2192-2197.

Keskinbora, K.H., & Jameel, M.A. (2018). Nanotechnology Applications and Approaches in medicine: A Review. *Journal of Nanoscience and Nanotechnology Research* 2(2), 6.

Kaminski, S., Lawrence, A., & Trujillo, D. (2016). Structural use of bamboo: Part 1: Introduction to bamboo. *Structural Engineer* 94(8), 40-43.

Khan, I., Saeed, K., & Khan, I. (2017). Nanoparticles: Properties, applications and toxicities. *Arabian Journal of Chemistry* (12), 908-931.

Li, B., Zhang, J., Ren, X., Chang, J., & Gou, J. (2014). Preparation and Characterization of Bio-Oil Modified Urea-Formaldehyde Wood Adhesives. *BioResources,* 9(3), 5125-5133.

Liu, G., Zheng, H., Jiang, Z., Zhao, J., Wang, Z., & Pan, B. (2018). Formation and physicochemical characteristics of Nano Biochar; insight into chemical and colloidal stability. *Environmental Science and Technology*, 52, 10369-10379.

Lubis, M., Park, B., & Lee, S. (2018). Modification of Urea-formaldehyde resin adhesives with blocked Isocyanates using sodium bisulfite. *International Journal of Adhesion and Adhesives* (73) 118-124.

Lusiani, R., Saefuloh, I., Listijorini, E., Sumarna, A.E., Fawaid, M., & Meliana, Y. (2020). Particleboard characterization using sawdust from sengon wood, mahogany wood, bayur wood, and rice husk ash as composite fillers. *International Conference on Advanced Mechanical and Industrial Engineering series: Materials Science and Engineering* 909(1), 012028.

Mahanim, S.M.A., Asma, I.W., Rafidah, J., Puad, E., & Shaharuddin, H. (2011). Production of Activated carbon from Industrial bamboo wastes. *Journal of Tropical Forest Science,* 23(4), 417-424

Mahardika, M., Abral, H., Kasim, A., Arief, S. & Asrofi, M. (2018). Production of Nanocellulose from pineapple leaf fibres via High Shear Homogenization and Ultrasonication. *Fibers* 6(2), 28.

Mary, G., Sugumaran, P., Niveditha, S., Ramalakshmi, B., Ravichandran, P., & Seshadri, S. (2016). Production, characterization and evaluation of biochar from pod (*Pisum sativum*), leaf (*Brassica oleracea*) and peel (*Citrus sinensis*) wastes. *International Journal of Recycling of Organic Waste in Agriculture,* 5(1), 43–53.

Matykiewicz, D. (2020). Biochar as an effective filler of carbon fiber reinforced bio-epoxy composites. *Processes,* 8(6), 724.

Melo, R., Stangerlin, D.M., Santana, R., & Pedrosa, T.D. (2014). Physical and Mechanical Properties of Particleboard Manufactured from Wood, Bamboo and Rice Husk. *Materials Research* 17(3), 682-686.

Mena, L., Pecora, A., & Beraldo, A. (2014). Slow pyrolysis of Bamboo Biomass: Analysis of Biochar properties. *Chemical Engineering Transactions,* 37, 115-120.

Mohammed, L., Ansari, M., Pua, G., Jawaid, M. & Islam, M. (2015). A Review of Natural Fibre Reinforced polymer composite and its Applications. *International Journal of Polymer Science.*

Muigai, H., Bordoloi, U., Hussain, R., Ravi, K., Moholka, V., & Kalita, P (2020). A comparative study on synthesis and characterization of biochars derived from lignocellulosic biomass for their candidacy in agronomy and energy applications. *International Journal of Energy Research.* 45(3), 4765-4781.

Nagavally, R.R. (2016). Composite Materials - History, Types, Fabrication Techniques, Advantages, and Applications. *International Journal of Advances in Science Engineering and Technology,* 5(9), 82-87.

Nurdin, H., Fernanda, Y., & Handayani, M. (2018). Analysis of Tensile Strength the Fiber Bagasse Particles Board with Resin Adhesives. *Teknomekanik* 1(1) 1-5.

Nuryawan, A., & Park, B. (2014). Microstructure of cured Urea-formaldehyde Resins modified by Rubber latex emulsion after Hydrolytic Degradation. *J. Korean Wood Science and Technology* 42(5): 605-614.

Nuryawan, A., Park, B., & Singh, A.P. (2014). Penetration of Urea-formaldehyde resins with different formaldehyde/urea mole ratios into softwood tissues. *Wood Science Technology* 48, 889-902.

Ohalete, M. N., & Popoola, A. V. (2019). Urea-formaldehyde Resins Synthesis, Modification and Characterization. *IOSR Journal of Applied Chemistry* 12(8) 19-25.

Okerulu, I. O., Onyema, C. T., Onwukeme, V. I., & Ezeh, C. M. (2017). Assessment of phytochemicals, proximate and elemental composition of Pterocarpus soyauxii (Oha) leaves. *American Journal of Analytical Chemistry,* 8(06), 406.

Ormondroyd, G. A. (2015). Adhesives for wood composites. *Wood Composites* 47-66. Woodhead Publishing.

Osemeahon, S.A., Barminas, J.T., & Aliyu, B.A. (2007). Effect of urea formaldehyde viscosity on some physical properties of a composite from reactive blending of

urea formaldehyde with natural rubber. *International Journal of Physical Sciences* 2(9), 242-248.

Ouarhim. W., Zari. N., Bouhfid. R. & Qaiss, A. (2019). Mechanical performance of natural fibres-based thermosetting composites. *Moroccan Foundation for Advanced Science, Innovation and Research (MAScIR)*

Oyedun, A., Gebreegziabher, T., & Hui, C. (2012). Mechanism and Modeling of bamboo pyrolysis. *Fuel processing Technology*. 106, 595-604.

Pal, S.L., Jana, U., Manna, P.K., Mohanta, G.P., & Manavalan, R. (2011). Nanoparticle: An overview of preparation and characterization. *Journal of Applied Pharmaceutical Science* 01 (06), 228-234.

Patel, S., & Amin, S. (2013). Urea-formaldehyde and Alkylated Urea formaldehyde review paper. *International Journal of Research in Information Technology*, 1(4), 1-11.

Petridis, L.V., Kokkinos, N.C., Mitropoulos, A.C., & Kyzas, G.Z. (2019). Graphene aerogels for oil absorption. *Interface Science and Technology*. (30), 173-197.

Peep, C., Tonis, P., & Kadri, S. (2006). Structure formation in urea-formaldehyde resin synthesis. *In Proceedings of the Estonian Academy of Sciences. Chemistry* 55(4), 212-225.

Park, B., & Causin, V., (2013). Crystallinity and domain size of cured Urea-formaldehyde Resin Adhesives with different formaldehyde/urea mole ratios. *European Polymer Journal* (49) 532-537.

Park, B., & Jeong, H. (2011)[a]. Hydrolytic stability and crystallinity of cured Urea-formaldehyde resin adhesives with different formaldehyde/urea mole ratios. *International Journal of Adhesion and Adhesives* (31), 524-529.

Park, B., & Jeong, H. (2011)[b]. influence of hydrolytic degradation on the morphology of cured Urea-formaldehyde Resins of different formaldehyde/urea mole ratios. *Mokchae Konghak* 39(2): 179-186.

Patryk, O., Wieslawa, C., Aleksandra, B., Ewa, S., & Yong, S. (2016). Characterization of nanoparticles of Biochars from different Biomass. *Journal of Analytical and Applied Pyrolysis.* DOI: http://dx.doi.org/10.1016/j.jaap.2016.07.017.

Pecas, P., Carvalho, H., Salman, H., & Leite, M. (2018). Natural fibre composites and their Applications: A Review. *Journal of Composites Science* 2,66.

Phuakpunk, K., Chalermsinsuwan, B., & Assabumrungrat, S. (2020). Pyrolysis Kinetic Analysis of Biomasses: Sugarcane Residue, Corn Cob, Napier grass and their mixture. *Engineering Journal* 24(4), 19-31.

Rachtanapun, P., & Heiden, P. (2002). Thermoplastic polymers as modifiers for Urea formaldehyde (UF) wood Adhesives. Procedures for the preparation and characterization of thermoplastic modified UF suspensions. *Journal of Applied Polymer Science* (87), 890-897.

Roumeli, E., Papadopoulou, E., Pavlidou, E., Vourlias, G., Bikiaris, D., Paraskevopoulos, K.M., & Chrissafis, K. (2011). Synthesis, characterization and thermal analysis of urea-formaldehyde/Nano $SiO_2$ resins. *Thermochimica Acta* (527), 33-39.

Sajid, M. & Plotka-wasylka, J. (2020). Nanoparticles: Synthesis, characteristics and applications in analytical and other sciences. *Microchemical Journal* 154, 104623

Sadare, O.O., Daramola, M.O., & Afolabi, A.S. (2015). Preparation and Characterization of Nanocomposite Soy-Carbon Nanotubes (SPI/CNTs) Adhesive from Soy Protein Isolate. *Proceedings of the World Congress on Engineering* 2, 1-3.

Sahoo, S., Vijay, V., Chandra, R., & Kumar, H. (2021). Production and Characterization of Biochar produced from slow Pyrolysis of Pigeon pea stalk and bamboo. *Cleaner Engineering and Technology* 3, 100101.

Saletnik, B., Zagula, G., Bajcar, M., Tarapatskyy, M., Bobula, G., & Puchalski, C. (2019). Biochar as a Multifunctional Component of the Environment- A Review. *Applied Science,* 9, 1139.

Singh, A.P., Causin, V., Nuryawan, A., & Park, B. (2014). Morphological, chemical and crystalline features of Urea-formaldehyde resin cured in contact with wood. *European Polymer Journal* (56), 185-193.

Suman, S. & Gautam, S. (2017). Pyrolysis of coconut husk biomass: Analysis of its biochar properties, Energy Sources, Part A: Recovery, Utilization, and Environmental Effects, 39(8), 761-767.

Sun, Q., Hse, C., & Shupe, T.F. (2014). Effect of different catalysts on Urea-formaldehyde Resin synthesis. *Journal of Applied polymer science*, 131(16).

Tan, x., Liu, Y., Gu, Y., Xu, Y., Zeng, G., Hu, X., Liu, S., Wang, X., Liu, S., & Li, J., (2016). Biochar based nano composites for the decontamination of wastewater: A review. *Bioresource Technology*, 212, 318-333.

Van Dam, J.E.G., Elbersen, H.W., & Montaño, C.M.D. (2018). Bamboo Production for Industrial Utilization. Perennial Grasses for Bioenergy and Bioproducts. 175-216.

Wahab, R., Sulaiman, M.S., Ghani, R.S.M., Mokhtar, N., Don, S.M.M., & Samsi, H.W. (2018). Properties of Composite Boards Properties from Elaeis guineensis Empty Fruit Bunch. *Borneo Journal of Sciences and Technology*, 1(1), 53-61.

Wang, G., & Chen, F. (2017). Development of Bamboo fibre-based composites. *In Advanced High Strength Natural Fibre Composites in Construction.* 235-255. Wood head publishing.

Wild, P. (2015). Pyrolysis of bamboo vulgaris for fuels, chemicals and energy. *International Biomass Conference and Exposition, Minneapolis.*

Wu, L., Guo, J., Zhang, Z., & Zhao, S. (2017). Influence of Oxidized Starch and Modified Nano-SiO2 on Performance of Urea-Formaldehyde (UF) Resin. *Polymer (Korea)*, 41(1), 83-89.

Yong No, B., & Kim, M.G. (2004). Synthesis and properties of low level Melamine-modified Urea-Melamine-formaldehyde Resins. *Journal of Applied Polymer Science* (93), 2559-2569.

Zaman, C. Z., Pal, K., Yehye, W. A., Sagadevan, S., Shah, S. T., Adebisi, G. A., & Johan, R. B. (2017). Pyrolysis: a sustainable way to generate energy from waste. Pyrolysis; *IntechOpen:* Rijeka, Croatia, 1.

# APPENDICES

## APPENDIX A

### Calculation for moisture content

Moisture content = $\frac{(W1-W2)}{W1} * 100$

Where;

W1= Weight of sample before drying (g)

W2= Weight of sample after drying (g)

### Calculation for ash content

Ash content = $\frac{W1}{W2}$

Where;

W1= Weight of ash

W2= Weight of dry sample

### Calculation for Volatile matter

Percentage volatile matter = $\frac{(W1-W2)}{W1} * 100$

Where;

W1= Weight of sample before drying (g)

W2= Weight of sample after drying (g)

**Calculation for fixed carbon content (FCC)**

Percentage FCC= $100-(ash$ content + volatile matter content + moisture content) %

**Calculation for density**

$\rho = \frac{M}{V}$

Where;

$\rho$ = Density ($g/cm^3$)

M= mass (g)

V= volume ($cm^3$)

**Calculation for volume**

$l*b*h$

Where;

l= length (mm)

b= breath (mm)

h= height (mm)

**Calculation for water absorption**

Water absorption (%) = $\frac{(Wf-Wi)}{Wi} * 100$

Where;

Wi= initial weight (g)

Wf= final weight (g)

**Calculation for thickness swelling**

Thickness swell (%) = $\frac{(Tf-Ti)}{Ti} * 100$

Where;

Ti = initial thickness (mm)

Tf = final thickness (mm)

## APPENDIX B

**Table B1: Water Absorption of particle boards**

| Samples | Water Absorption (%) | | |
|---|---|---|---|
| | First reading | Second reading | Third reading |
| S0 | 37.2 | 35.5 | 38.4 |
| S1 | 38 | 30.4 | 36.8 |
| S2 | 30.4 | 34 | 31.8 |
| S3 | 35.8 | 34.5 | 31.2 |

**Table B2: Thickness Swell of particle boards**

| Samples | Thickness Swell (%) | | |
|---|---|---|---|
| | First reading | Second reading | Third reading |
| S0 | 46.5 | 47.5 | 45.8 |
| S1 | 42 | 45.2 | 42.6 |
| S2 | 39 | 41.5 | 41 |
| S3 | 42.8 | 45.9 | 41.8 |

**Table B3: Hardness of particleboards**

| Samples | Hardness HV | | |
|---|---|---|---|
| | First reading | Second reading | Third reading |
| S0 | 23.4 | 22.5 | 24.2 |
| S1 | 25.2 | 26.3 | 24.4 |
| S2 | 30.3 | 27.6 | 29.4 |
| S3 | 44 | 46.7 | 44 |

**Table B4: Impact of particle boards**

| Samples | Impact (J) | | |
|---|---|---|---|
| | First reading | Second reading | Third reading |
| S0 | 0.25 | 0.3 | 0.2 |
| S1 | 0.25 | 0.2 | 0.2 |
| S2 | 0.26 | 0.27 | 0.3 |
| S3 | 0.2 | 0.25 | 0.5 |

## Appendix C

### Tensile properties of particleboard sample S0

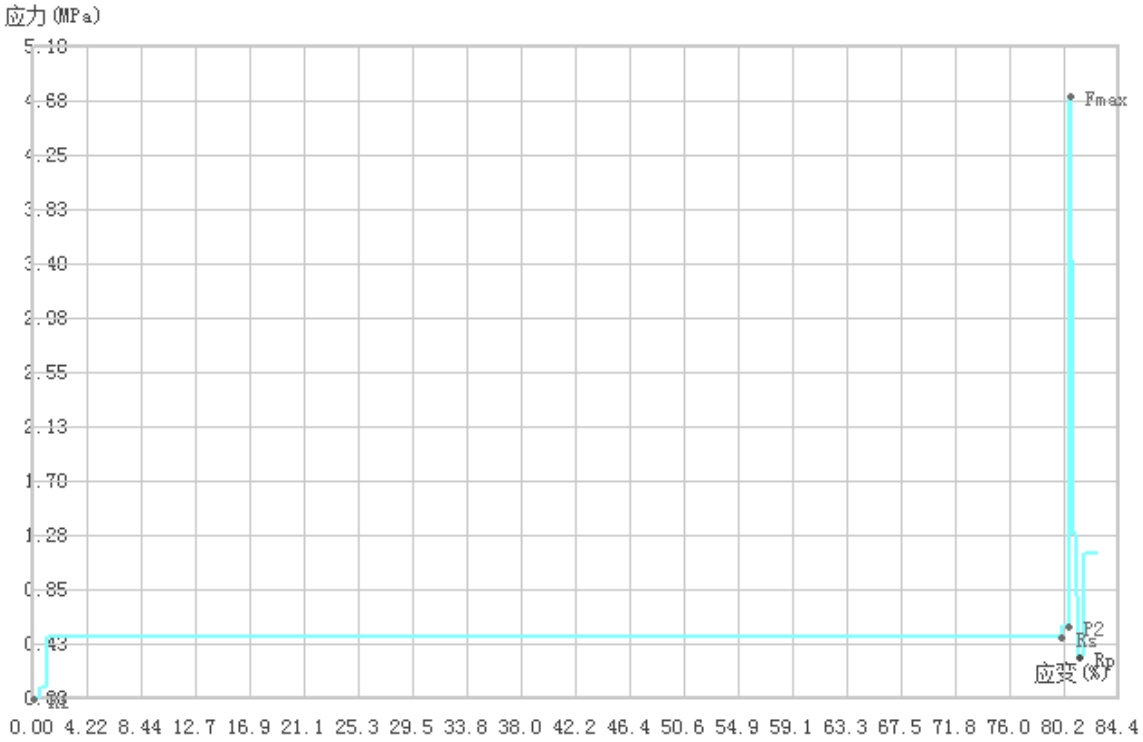


**Figure C1: 1st Stress-strain graph for sample S0**

| | | | |
|---|---|---|---|
| Elastic Modulus | 0.75MPa | Upper Yield | 0.00MPa |
| Yield Strength | 0.48MPa | Break Strength | 1.12MPa |
| Break Elongation | 82.73% | Elongation after fracture | 82.73% |
| Total Elongation | 80.68% | Yield Elongation | 79.92% |
| Yield Ratio | 10.17% | MaxLoad | 0.24kN |
| Max Elong | 33.09mm | Lower Yield | 0.00MPa |
| Tensile Strength | 4.72MPa | Reduction of Area | 100.00% |
| Non Proport Elongation | 0.76% | | |

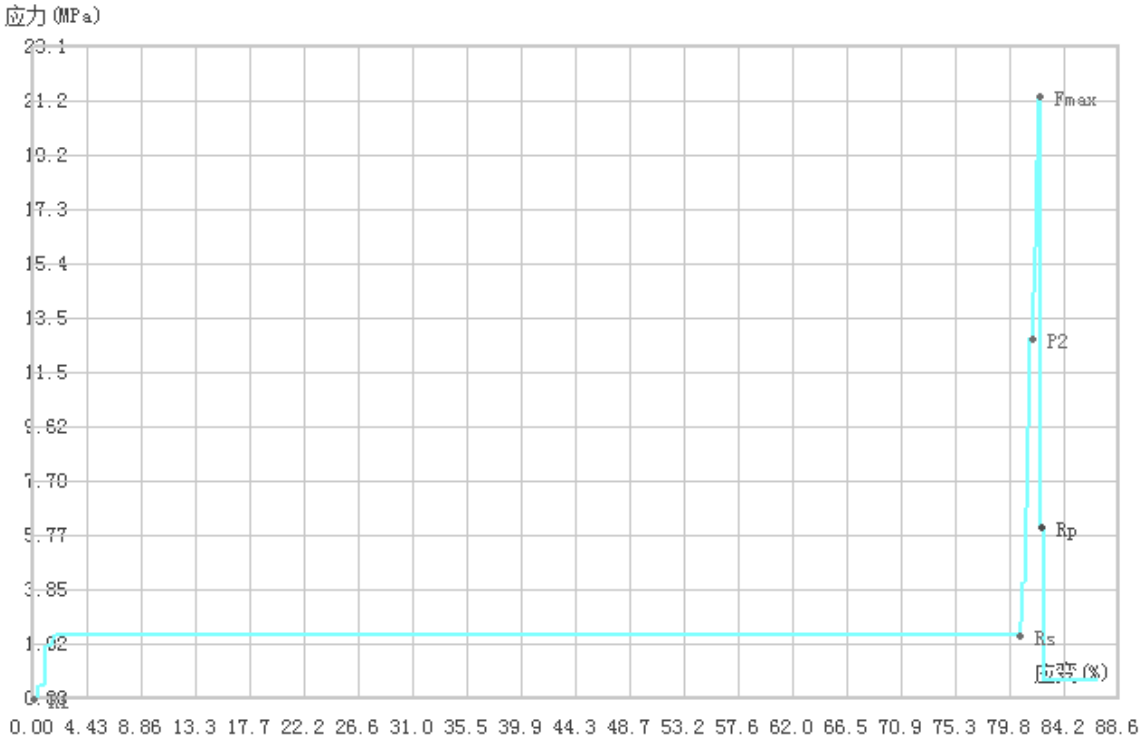


**Figure C2: 2nd Stress-Strain graph for sample S0**

| | | | |
|---|---|---|---|
| Elastic Modulus | 15.67MPa | Upper Yield | 0.00MPa |
| Yield Strength | 2.24MPa | Break Strength | 0.64MPa |
| Break Elongation | 86.86% | Elongation after fracture | 86.86% |
| Total Elongation | 82.17% | Yield Elongation | 80.60% |
| Yield Ratio | 10.49% | Max Load | 1.07kN |
| Max Elong | 34.74mm | Lower Yield | 0.00MPa |
| Tensile Strength | 21.36MPa | Reduction of Area | 100.00% |
| Non Proport Elongation | 1.56% | | |

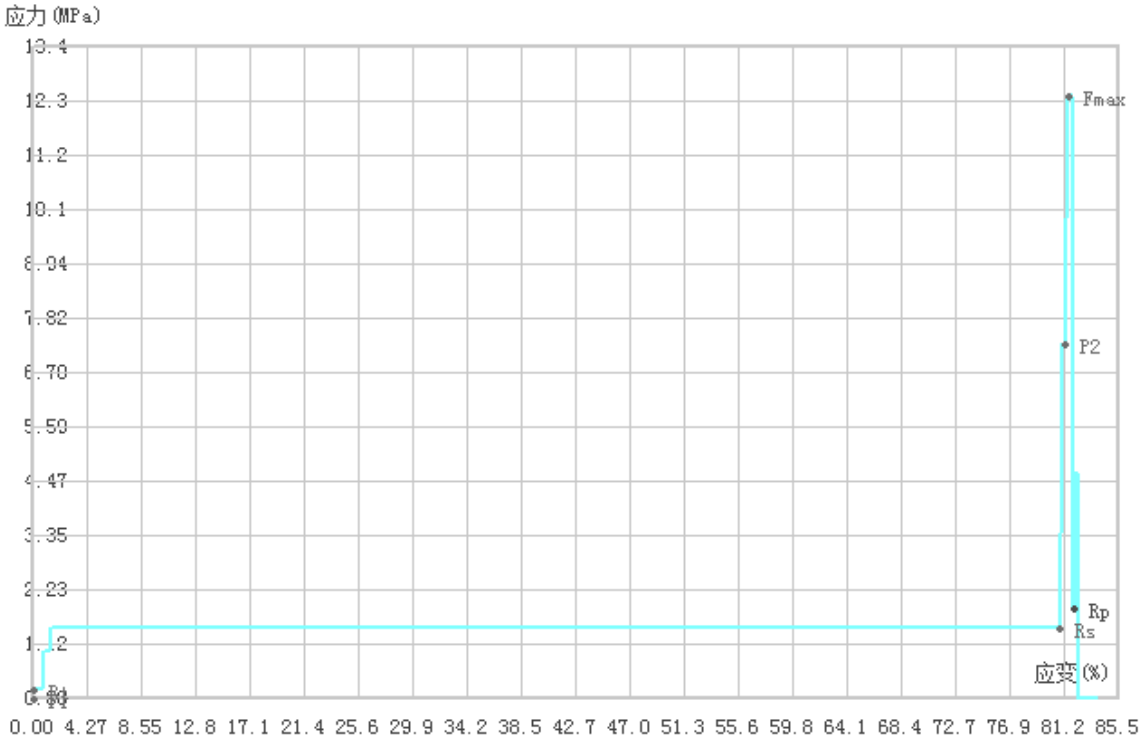


**Figure C3: 3rd Stress-Strain graph for sample S0**

| | | | |
|---|---|---|---|
| Elastic Modulus | 8.86MPa | Upper Yield | 0.00MPa |
| Yield Strength | 1.44MPa | Break Strength | 4.64MPa |
| Break Elongation | 83.61% | Elongation after fracture | 83.77% |
| Total Elongation | 81.57% | Yield Elongation | 80.80% |
| Yield Ratio | 11.61% | Rt0.2 | 0.16MPa |
| Max Load | 0.62kN | Max Elong | 33.51mm |
| Lower Yield | 0.00MPa | Tensile Strength | 12.40MPa |
| Reduction of Area | 100.00% | Non Proport Elongation | 0.76% |

**Tensile Properties of particleboard sample S1**

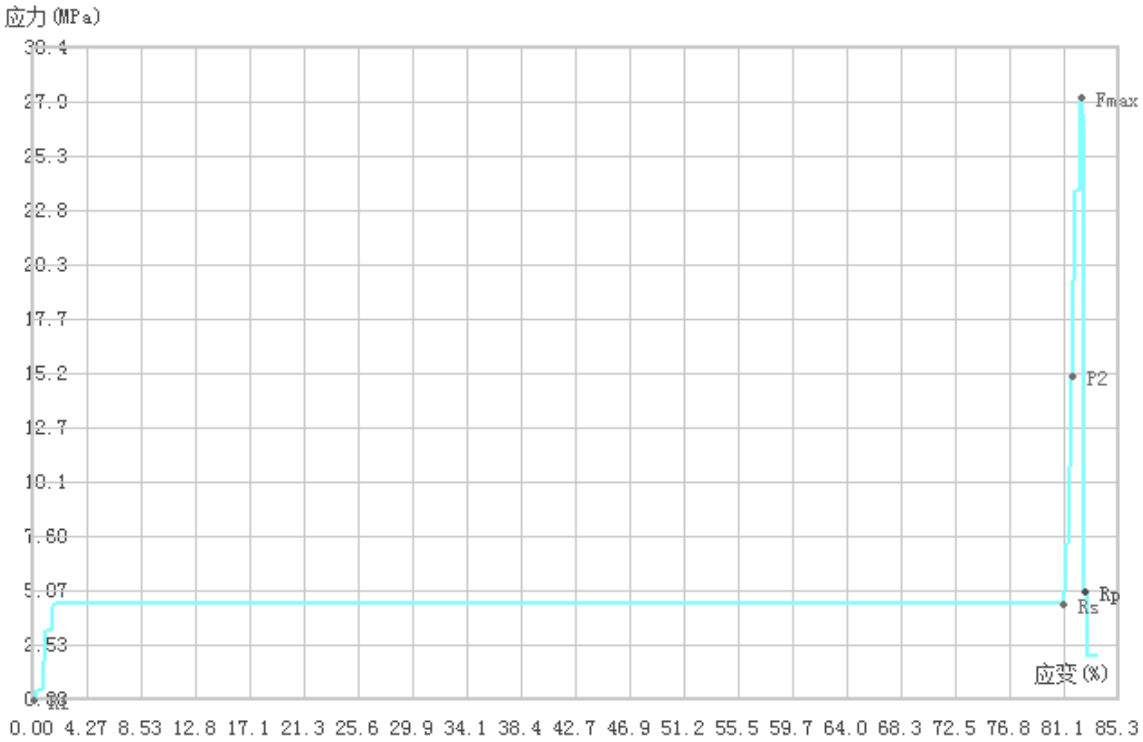


**Figure C4: 1st Stress-Strain graph for sample S1**

| | | | |
|---|---|---|---|
| Elastic Modulus | 18.35MPa | Upper Yield | 0.00MPa |
| Yield Strength | 4.40MPa | Break Strength | 2.00MPa |
| Break Elongation | 83.61% | Elongation after fracture | 83.61% |
| Total Elongation | 82.37% | Yield Elongation | 80.96% |
| Yield Ratio | 15.64% | MaxLoad | 0.84kN |
| Max Elong | 33.44mm | Lower Yield | 0.00MPa |
| Tensile Strength | 28.13MPa | Reduction of Area | 100.00% |
| Non Proport Elongation | 1.40% | | |

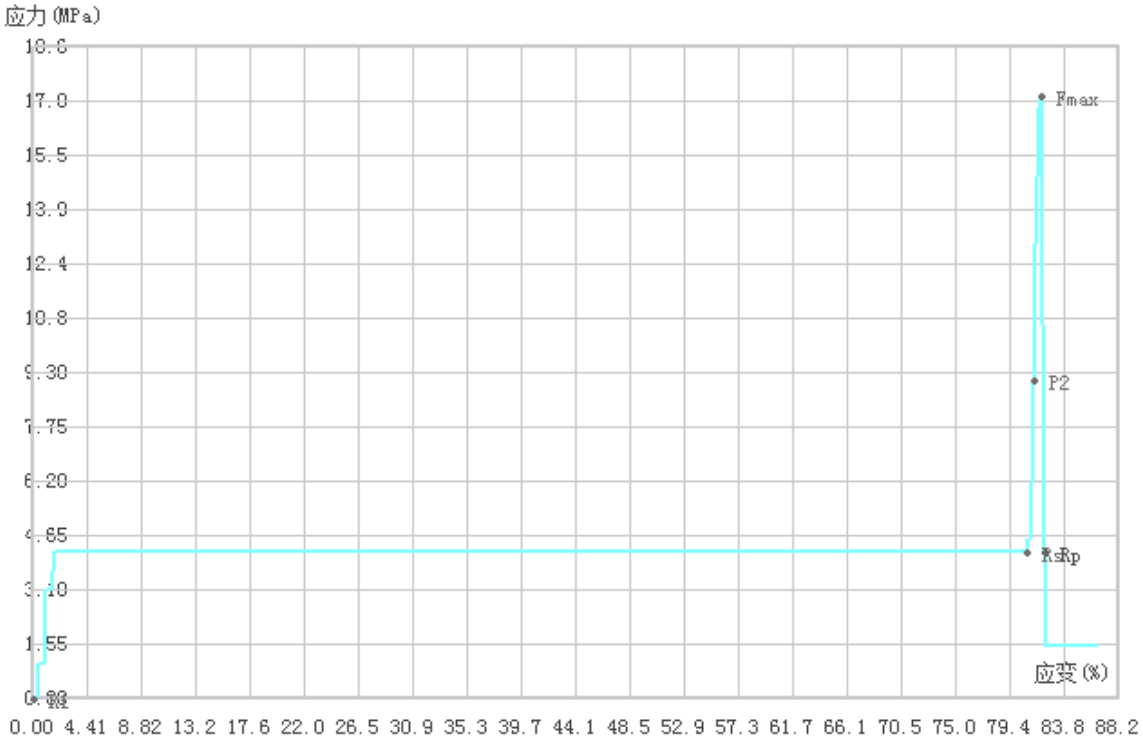


**Figure C5: 2nd Stress-Strain graph for sample S1**

| | | | |
|---|---|---|---|
| Elastic Modulus | 11.06MPa | Upper Yield | 0.00MPa |
| Yield Strength | 4.13MPa | Break Strength | 1.47MPa |
| Break Elongation | 86.42% | Elongation after fracture | 86.42% |
| Total Elongation | 82.01% | Yield Elongation | 80.76% |
| Yield Ratio | 24.03% | Max Load | 0.52kN |
| Max Elong | 34.57mm | Lower Yield | 0.00MPa |
| Tensile Strength | 17.20MPa | Reduction of Area | 100.00% |
| Non Proport Elongation | 1.24% | | |

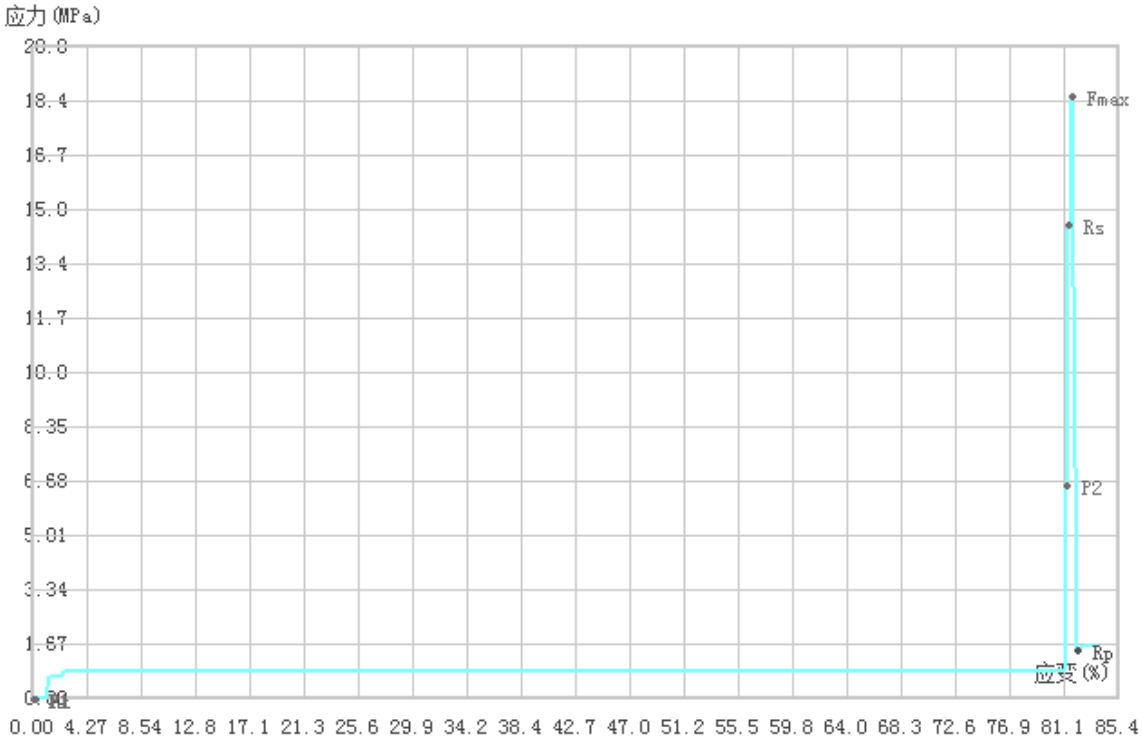


**Figure C6: 3rd Stress-Strain graph for sample S1**

| | | | |
|---|---|---|---|
| Elastic Modulus | 8.19MPa | Upper Yield | 0.00MPa |
| Yield Strength | 14.53MPa | Break Strength | 1.60MPa |
| Break Elongation | 83.69% | Elongation after fracture | 83.69% |
| Total Elongation | 81.81% | Yield Elongation | 81.52% |
| Yield Ratio | 78.42% | Max Load | 0.56kN |
| Max Elong | 33.48mm | Lower Yield | 0.00MPa |
| Tensile Strength | 18.53MPa | Reduction of Area | 100.00% |
| Non Proport Elongation | 0.28% | | |

**Tensile properties of particleboard sample S2**

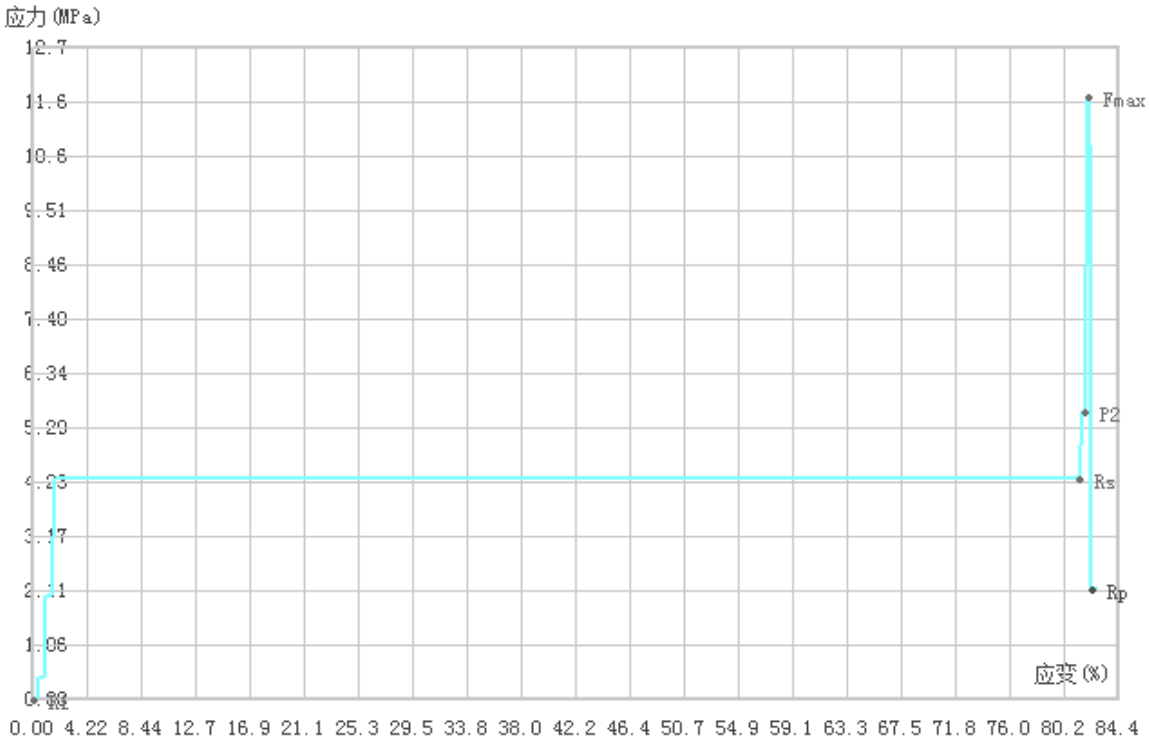


**Figure C7: 1st Stress-Strain graph for sample S2**

| | | | |
|---|---|---|---|
| Elastic Modulus | 6.93MPa | Upper Yield | 0.00MPa |
| Yield Strength | 4.27MPa | Break Strength | 2.13MPa |
| Break Elongation | 82.73% | Elongation after fracture | 82.73% |
| Total Elongation | 82.09% | Yield Elongation | 81.45% |
| Yield Ratio | 36.36% | MaxLoad | 0.35kN |
| Max Elong | 33.09mm | Lower Yield | 0.00MPa |
| Tensile Strength | 11.73MPa | Reduction of Area | 100.00% |
| Non Proport Elongation | 0.64% | | |

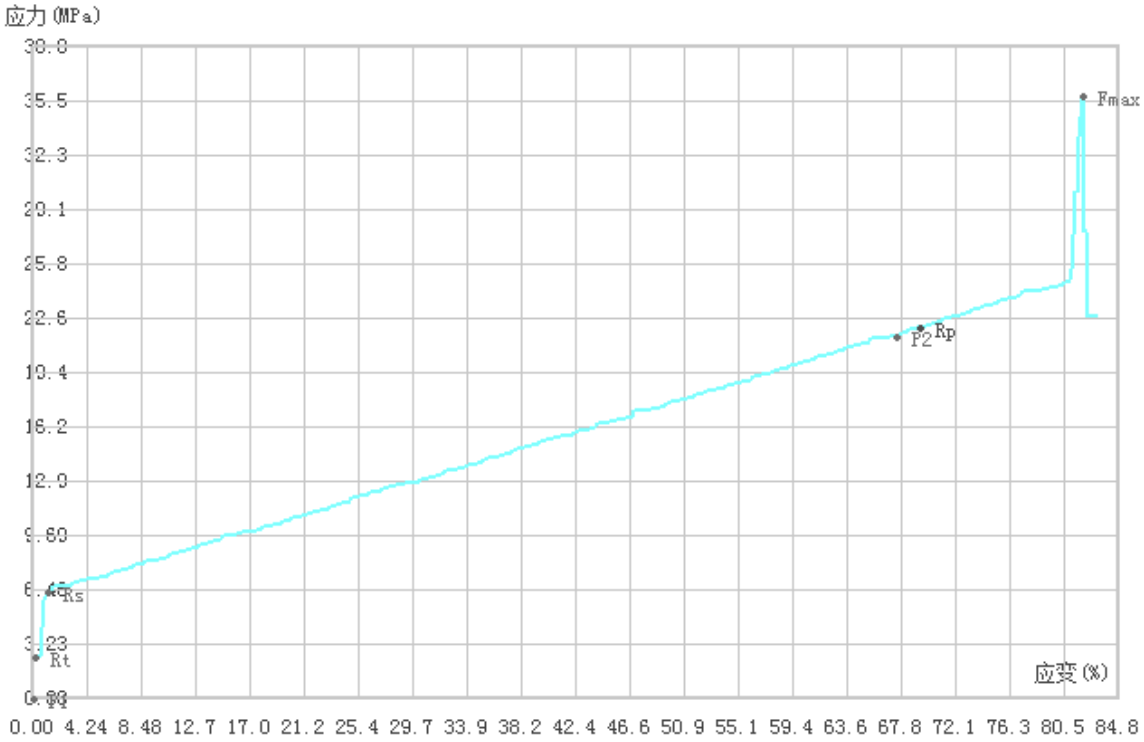


**Figure C8:2nd Stress-Strain graph for sample S2**

| | | | |
|---|---|---|---|
| Elastic Modulus | 31.65MPa | Upper Yield | 0.00MPa |
| Yield Strength | 6.27MPa | Break Strength | 22.67MPa |
| Break Elongation | 83.09% | Elongation after fracture | 83.09% |
| Total Elongation | 81.97% | Yield Elongation | 1.13% |
| Yield Ratio | 17.47% | Max Load | 1.08kN |
| Max Elong | 33.24mm | Lower Yield | 0.00MPa |
| Tensile Strength | 35.87MPa | Reduction of Area | 100.00% |
| Non Proport Elongation | 80.84% | | |

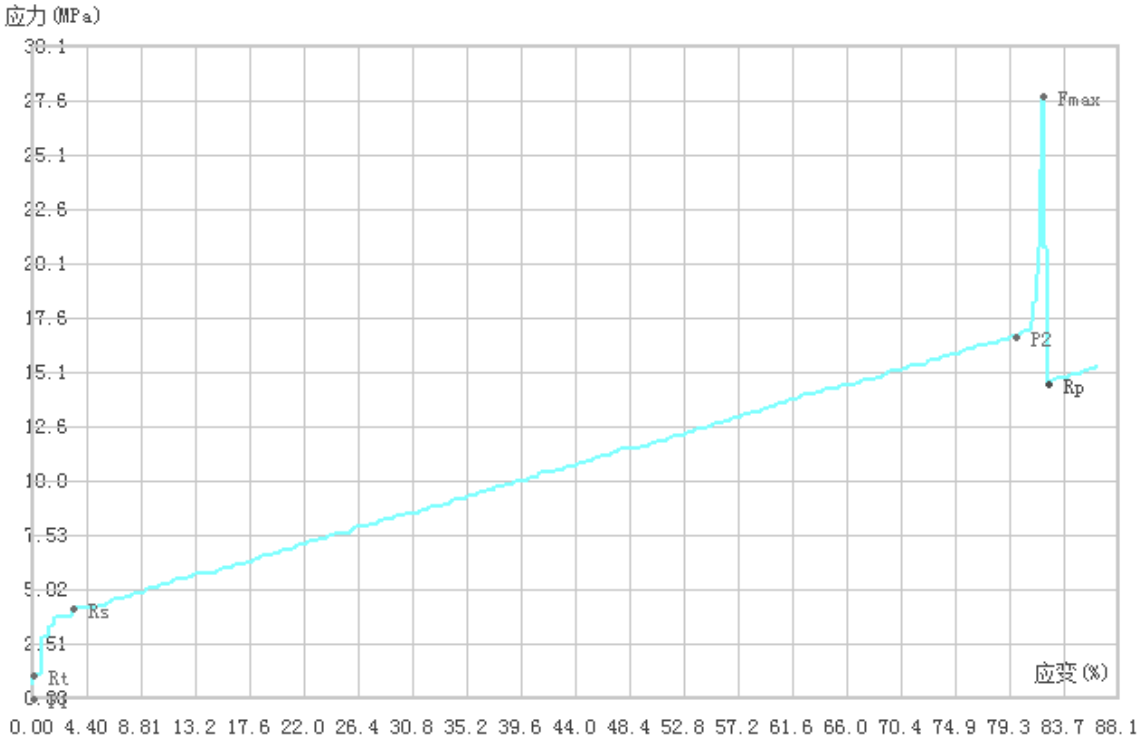


**Figure C9: 3rd Stress-Strain graph for sample S2**

| | | | |
|---|---|---|---|
| Elastic Modulus | 20.91MPa | Upper Yield | 0.00MPa |
| Yield Strength | 4.13MPa | Break Strength | 15.33MPa |
| Break Elongation | 86.30% | Elongation after fracture | 86.30% |
| Total Elongation | 81.93% | Yield Elongation | 3.26% |
| Yield Ratio | 14.83% | Max Load | 0.84kN |
| Max Elong | 34.52mm | Lower Yield | 0.00MPa |
| Tensile Strength | 27.87MPa | Reduction of Area | 100.00% |
| Non Proport Elongation | 78.67% | | |

**Tensile properties of particleboard sample S3**

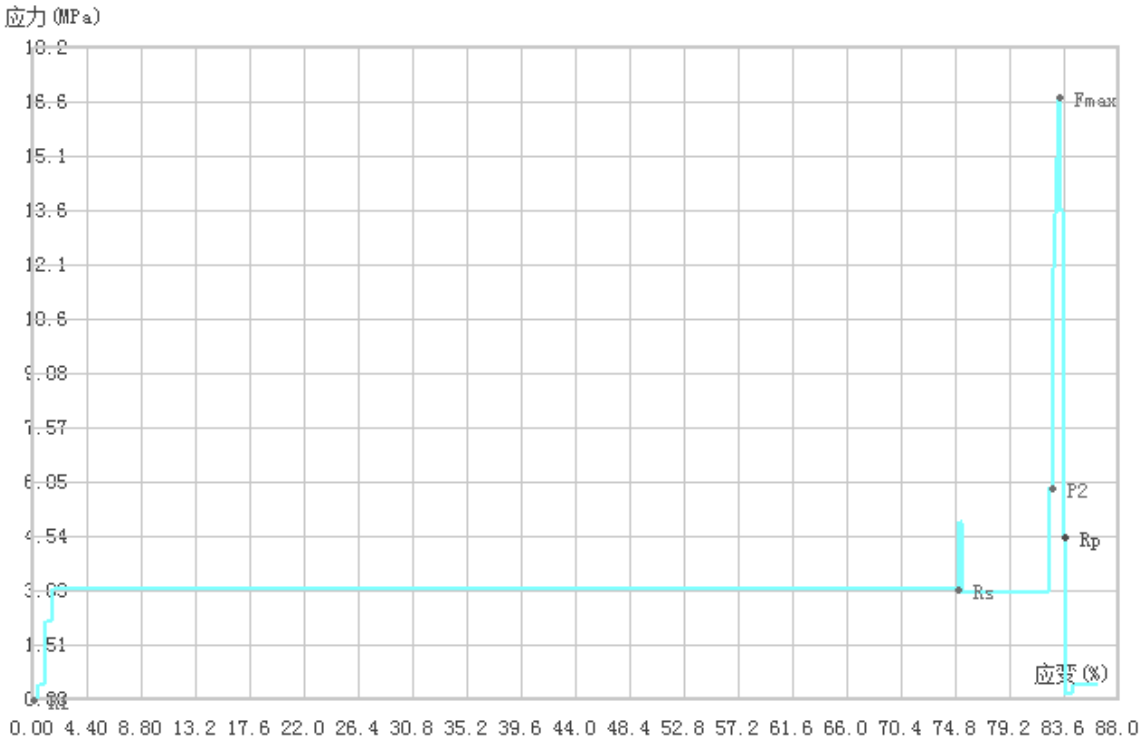


**Figure C10: 1st Stress-Strain graph for sample S3**

| | | | |
|---|---|---|---|
| Elastic Modulus | 7.25MPa | Upper Yield | 0.00MPa |
| Yield Strength | 3.07MPa | Break Strength | 0.40MPa |
| Break Elongation | 86.25% | Elongation after fracture | 86.25% |
| Total Elongation | 83.20% | Yield Elongation | 74.98% |
| Yield Ratio | 18.25% | MaxLoad | 0.50kN |
| Max Elong | 33.64mm | Lower Yield | 0.00MPa |
| Tensile Strength | 16.80MPa | Reduction of Area | 100.00% |
| Non Proport Elongation | 8.23% | | |

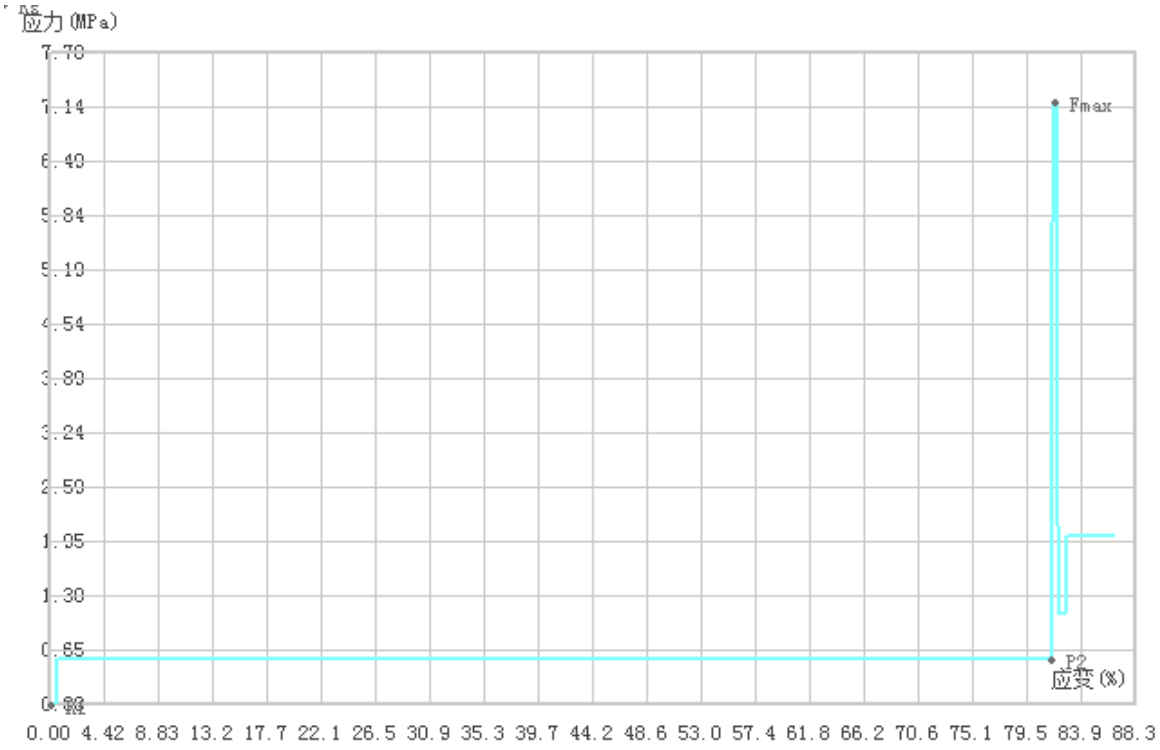


**Figure C11: 2nd Stress-Strain graph for sample S3**

| | | | |
|---|---|---|---|
| Elastic Modulus | 0.82MPa | Upper Yield | 0.00 MPa |
| Yield Strength | 0.00MPa | Break Strength | 2.00 MPa |
| Break Elongation | 86.54% | Elongation after fracture | 86.54% |
| Total Elongation | 81.72% | Yield Elongation | 0.00 % |
| Yield Ratio | 0.00% | Max Load | 0.22 kN |
| Max Elong | 33.75mm | Lower Yield | 0.00 MPa |
| Tensile Strength | 7.20MPa | Reduction of Area | 100.00% |
| Non Proport Elongation | 2373323880751739300000000000000000000000000000000000000000.00% | | |

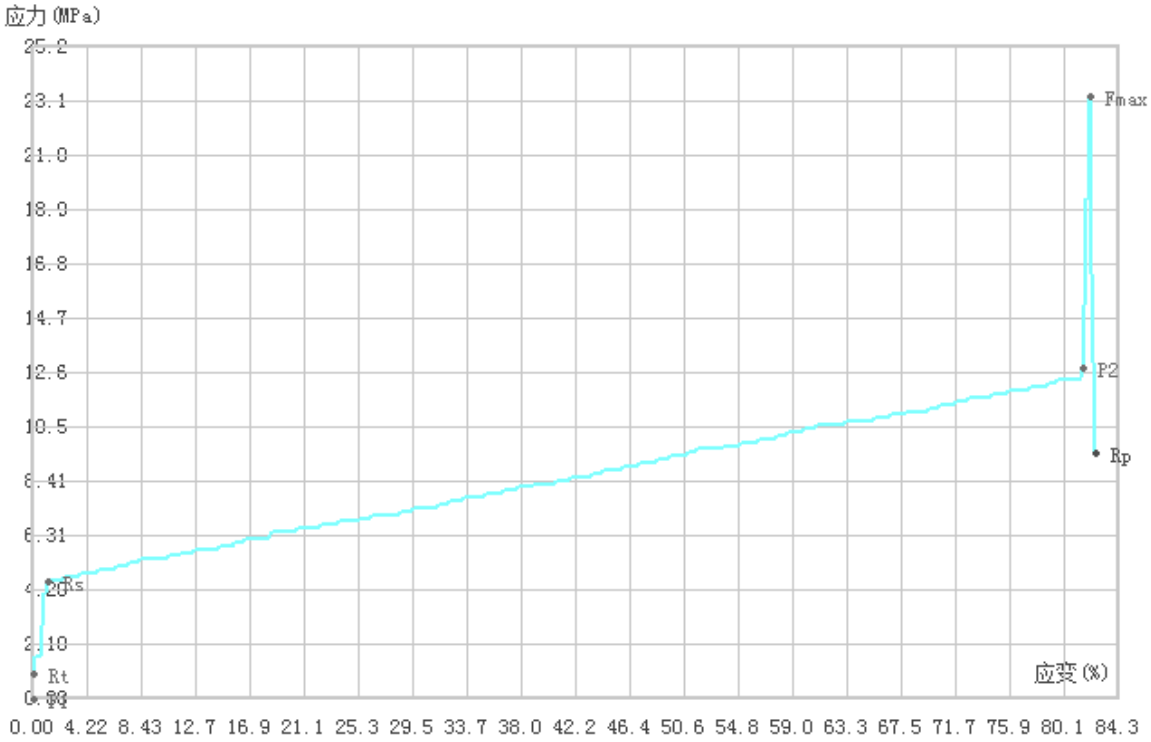


**Figure C12: 3rd Stress-Strain graph for sample S3**

| | | | |
|---|---|---|---|
| Elastic Modulus | 15.53MPa | Upper Yield | 0.00MPa |
| Yield Strength | 4.53MPa | Break Strength | 9.47MPa |
| Break Elongation | 82.65% | Elongation after fracture | 82.65% |
| Total Elongation | 82.21% | Yield Elongation | 1.17% |
| Yield Ratio | 19.43% | MaxLoad | 0.70kN |
| Max Elong | 33.06mm | Lower Yield | 0.00MPa |
| Tensile Strength | 23.33MPa | Reduction of Area | 100.00% |
| Non Proport Elongation | 81.04% | | |